Bachelor's thesis

Bachelor's degree in Industrial Technologies and Economic Analysis

Simulation of Electric Vehicle performance considering battery degradation

REPORT

September 12, 2023

Author: Alba Lun Mora Pous

Director: Maite Etxandi Santolaya

Call: September 2023

Escola Tècnica Superior
d'Enginyeria Industrial de Barcelona

Abstract

[ENG] Electromobility has emerged as a promising alternative to combat the environmental impact of internal combustion engine (ICE) vehicles. The most important part of an Electric Vehicle (EV) is the battery, as it is the component which determines its performance. Battery end-of-life is conventionally associated with a decline in performance characterized by increased internal resistance (IR) and a State of Health (SOH) below 80%. Below this threshold, a battery is often considered not suitable for use. This thesis conducts simulations to assess EV performance while considering battery degradation. The study evaluates five distinct driving cycles across varying battery conditions and road scenarios. Findings reveal that batteries with lower SOH levels can still perform effectively, particularly in low-demand driving scenarios and on flat terrains. The ability to extend the lifespan of batteries, even as they degrade, has the potential to yield economic benefits and reduce the environmental footprint of battery production and disposal. This study tries to emphasize the importance of optimizing battery usage in the pursuit of sustainable electromobility solutions.

[CAT] L'electromobilitat ha emergit com a una alternativa prometedora per combatre l'impacte mediambiental provocat pels vehicles de combustió interna. La part més important dels vehicles elèctrics (EV) és la bateria, ja que és el component que determina el rendiment del VE. El final de la vida útil d'una bateria està associat amb una disminució d'aquest rendiment, el qual està caracteritzat per un increment en la resistència interna (RI) i un estat de salut inferior al 80%. Per sota d'aquest límit, una bateria és generalment considerada com a no apte per la seva utilització. Aquesta tesi consisteix en dur a terme simulacions per estudiar el rendiment d'un VE considerant la degradació de la bateria. L'estudi avalua 5 cicles de conducció diferents amb unes condicions variables de la bateria i la carretera. Els resultats suggereixen que les bateries amb menys estat de salut poden funcionar correctament, especialment en cicles de conducció poc exigents i en carreteres planes. El fet de poder allargar la vida útil de les bateries tot i que estiguin degradades pot resultar en beneficis econòmics i reduir la petjada ecològica causada per la producció de les bateries i els residus associats a aquestes. Aquest estudi intenta posar èmfasi en la importància d'optimitzar l'ús de les bateries elèctriques per poder aconseguir solucions sostenibles relacionades amb l'electromobilitat.

[CAS] La electromovilidad ha emergido como una alternativa prometedora para combatir el impacto medioambiental provocado por los vehículos de combustión interna. La parte más importante de los vehículos eléctricos (VE) es la batería, puesto que es el componente que determina su rendimiento. El final de vida útil de la batería está asociado con una disminución de este rendimiento caracterizado por un incremento de la resistencia interna (RI) y un estado de salud inferior al 80%. Por debajo de este límite, una batería es generalmente considerada como no adecuada para su uso. Esta tesis consiste en realizar simulaciones para estudiar el rendimiento de un VE teniendo en cuenta la degradación de la batería. El estudio evalúa 5 ciclos de conducción distintos con unas condiciones variables de la batería y de la carretera. Los resultados sugieren que las baterías con menos estado de salud pueden funcionar correctamente, especialmente en ciclos de conducción poco exigentes y en carreteras planas. Poder alargar la vida útil de las baterías aun cuando tienen degradación, puede resultar en beneficios económicos y reducir la huella ecológica causada por la producción de las baterías y los residuos asociados a ellas. Este estudio intenta recalcar la importancia de optimizar el uso de las baterías eléctricas para poder alcanzar soluciones sostenibles relacionadas con la electromovilidad.

Contents

List of Figures

List of Tables

1 Preface

1.1 Origin of the project

Environmental concerns have arisen during the last century due to the increasing levels of industrial activity, burning of fossil fuels and release of greenhouse gases. It is estimated that transport accounts for approximately 26% of the global CO_2 emissions [5], which has resulted in the gradual replacement of internal combustion engine (ICE) vehicle by the electric vehicle (EV).

The increasing popularity of EV and their associated emerging market are the reason why manufacturers dedicated to their development are encountering the urge to study and improve such machines' performance. In the context of EVs, especial focus on battery is placed as this is the component that determines the overall vehicle performance.

1.2 Background

EVs can be mainly divided into battery electric vehicles (BEV), hybrid electric vehicles (HEV) and plug-in-hybrid electric vehicles (PHEV). The remarkable difference between them is that BEV are 100% propelled by electric power drawn by the motor from the electric battery, while HEV and PHEV are formed by a combination of both ICE and an electric motor. In all EVs, batteries play an essential role since it is what establishes how far will the car travel without it needing to be charged (analogous to fuel tank in cars with only ICE).

More precisely, EVs rely on the electricity provided by their battery for traction. These batteries suffer from an unavoidable degradation process that generates two effects: a loss in the capacity and an increase in the Internal Resistance (IR) [10]. This degradation is influenced by many factors, being the temperature, current, number of charging/discharging cycles, etc. the ones that make greater impact.

Degradation can lead to unpredictable and/or unwanted battery behaviour and lower vehicle performance. Consequently, battery is considered not suitable for use when reaching end-of-life, which is conventionally characterized by State of Health (SOH) below 80%.

2 Introduction

2.1 Objectives of the project

The aim of the study is to understand the limitations in driving that a user might face as the battery degrades and SOH levels decrease, with especial focus on evaluating how the increase in IR may limit functional aspects like driving at high speeds, sudden accelerations or driving uphill.

2.2 Project scope

The absence of an ICE makes the battery to play a very critical role in BEV, unlike in hybrid models where the presence of an ICE allows for the vehicle to have less dependency on the electric motor and battery. For this reason, the study in this thesis is mainly focused on BEV, to which are referred from now on as simply EVs. First, it is important to begin by describing the state of the art and putting in context EVs and their elements such as the battery and the Battery Management System (BMS).

Focus is driven to Li-ion batteries since these are the battery type most present in the automotive market [9]. However, it is worth mentioning that other type of batteries can be conforming the battery of an EV, thus obtaining differing results to the ones in this thesis.

2.3 State of the art

2.3.1 Electric Vehicles

In 1881 the first EVs were created and were almost used only as taxies in metropolises. By 1900, Evs represented the 28% of the total vehicles but low oil prices made ICEs to finally conquer the market [31]. It took a while but, more than a century later, EVs have revolutionized the whole automotive sector and the transportation paradigm. The principal reasons of their success are their ecological benefits and their relatively low maintenance cost compared to regular ICEs [26].

A funcional and contemporary EV involves the interaction of many subsystems, being the ones exposed in Figure 1 the most important ones. For the purpose of this thesis, focus will be driven mainly on the Energy Source subsystem, and more specifically on Batteries.

2.3.2 Batteries

A battery is a device that obtains electrical energy from the conversion of chemical energy. It is composed by an arrangement of one or various electro-chemical cells that act as a source of electrical energy.

Since many types of batteries exist, there are many ways to classify them, such as by size, application, voltage or chemistry.

A common way to classify them by chemistry is by their chargeable characteristics. A primary battery is one that cannot be recharged, while a secondary battery has rechargeable qualities. Additionally, batteries can be chemically classified by distinguishing the materials that the battery cell is made of. Since the pile was invented by Alessandro Volta in 1799, many variety of electrical batteries have been developed. The most common types are the lithium, alkaline,

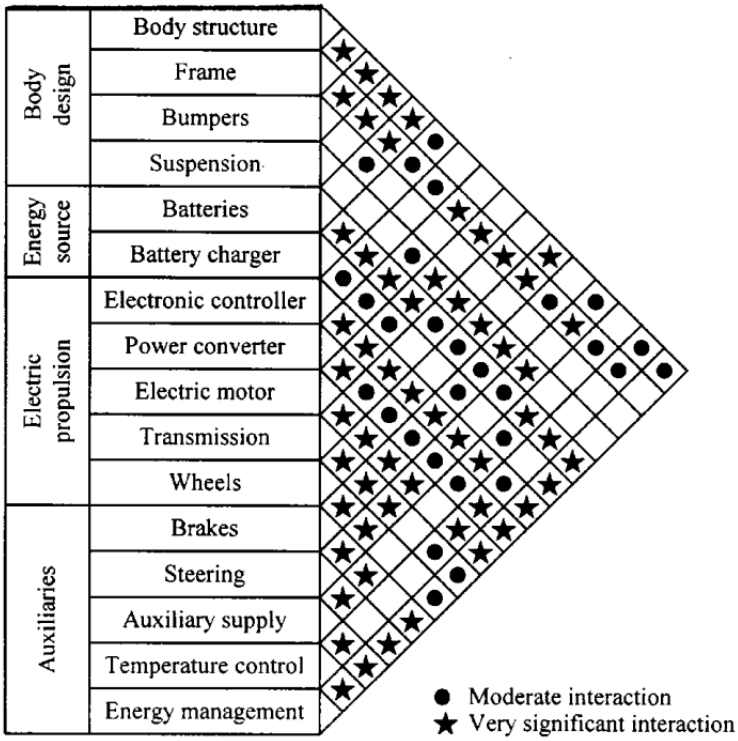

Figure 1: Interaction among EV subsystems [4]

carbon zinc and silver oxide for primary batteries; and lithium-ion (Li-ion), nickel cadmium (Ni-Cd), nickel metal hydride (NiMH) and lead-acid (Pb-acid) for secondary batteries [6]. In the automotive sector, the preferences lean towards the Li-ion secondary batteries.

The rechargeable characteristic is fundamental in an EV for very basic reasons: the battery is analogous to a fuel tank in ICEs. Therefore, after usage of the vehicle, energy is consumed from the battery. In order to "refill" the tank" (the battery in EV case), the battery needs to be electrically recharged whenever it is discharged if it is desired to make the vehicle functional again.

However, the choice of Li-ion is due to the advantages that it brings compared to the other options in the market. Li-ion batteries provide high voltage capacity and additionally they have a very convenient ratio of power output per unit of battery mass [9], which implies that they can hold more energy storage capacity than other battery types of same scale. This is particularly beneficial for cars, since the weight and dimensions highly impact the overall vehicle aerodynamics.

Additional technical specifications comparison has been summarized in Table 1, in which it is exposed additional advantageous characteristics of Li-ion versus other battery types such as their high-energy efficiency, no memory effects, and a relatively long cycle life [9].

Specifications	Lead acid	NiCd	NiMH	Li-ion		
				Cobalt	Manganese	Phosphate
Specific energy density (Wh/kg)	30–50	45–80	60–120	150–190	100–135	90–120
Internal resistance (mΩ)	<100 12 V pack	100–300 6 V pack	200–300 6 V pack	150–300 7.2 V	25–75 per cell	25–50 per cell
Cycle life (80% discharge)	200–300	1000	300–500	500–1000	500–1000	1000–2000
Fast charge time	8–16 h	1 h typical	2–4 h	2–4 h	1 h or less	1 h or less
Overcharge tolerance	High	Moderate	Low	Low. Cannot tolerate tickle charge		
Self-discharge/month (room temp.)	5%	20%	30%	<10%		
Cell voltage (nominal)	2 V	1.2 V	1.2 V	3.6 V	3.8 V	3.3 V
Charge cutoff voltage (V/cell)	2.40 Float 2.25	Full charge detection by voltage signature		4.20		3.60
Discharge cutoff voltage (V/cell, 1C)	1.75	1.00		2.50–3.00		2.80
Peak load current	5C	20C	5C	>3C	>30C	>30C
Best result	0.2C	1C	0.5C	>1C	<10C	<10C
Charge temperature	−20 to 50 °C (−4 to 122 °F)	0 to 45 °C (32 to 113 °F)		0 to 45 °C (32 to 113 °F)		
Discharge temperature	−20 to 50 °C (−4 to 122 °F)	−20 to 65 °C (-4 to 49 °F)		−20 to 60 °C (-4 to 140 °F)		
Maintenance requirement	3–6 months (topping charge)	30–60 days (discharge)	60–90 days (discharge)	Not required		
Safety requirements	Thermally stable	Thermally stable, fuse protection common		Protection circuit mandatory		
In use since	Late 1800s	1950	1990	1991	1996	1999
Toxicity	Very high	Very high	Low	Low		

Table 1: Comparison between different battery technologies [9].

Li-ion batteries are also present in the sector of consumer electronics & devices and the sector of grid energy & industry. Their high demand has allowed for mass production and a subsequent gradually cost reduction (from 2010 to 2016, costs have declined at a rate of almost 20% per year [8]). The combination of this, in conjunction with the previously mentioned issues, make Li-ion batteries the most competitive in the market and thus the type of battery that nowadays predominates in the EV battery industry [9].

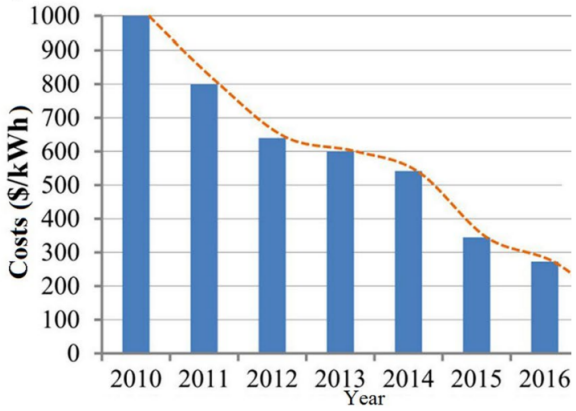

Figure 2: Cost evolution trend of Li-ion batteries from 2010 to 2016 [8]

Battery cells

A battery cell is composed primarily by an anode, a cathode, a current collector, an electrolyte and a separator. These components are the reason why the chemical reaction takes place.

A build up of electrons occur at the anode due to chemical reactions, which implies an electrical difference between the anode and the cathode. A discharge results from the movement of the electrons from the anode to the cathode in order to overcome this electrical difference. The larger this difference, the higher the voltage and the more energy that the battery can store. [2]

The separator is crucial so as to avoid short-circuiting when the ionic movement occurs, and the electrolyte function is to ensure that the electrons move with ease. Finally, the current collector is vital for transmitting the electricity generated by the flow of electrons to an external circuit. A typical cell format can be seen in Figure 3.

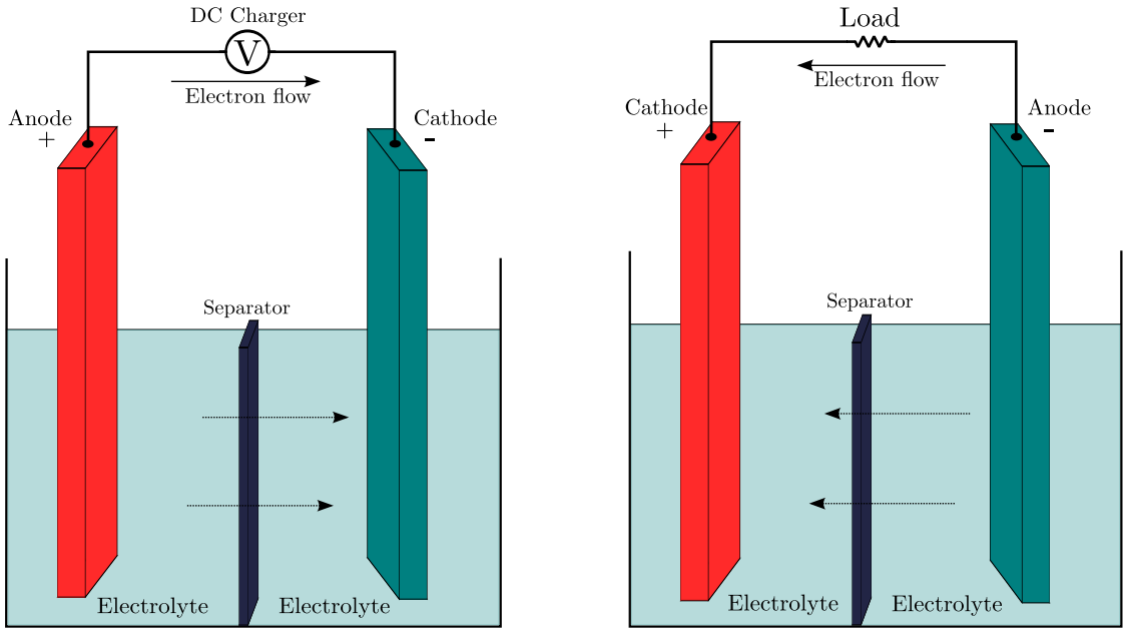

Figure 3: Typical cell format during charging and discharging [20]

Battery modules and battery packs

When high voltage is needed to be provided, individual battery cells are assembled together in series and parallel configurations in order to conform a single unit known as battery modules. Different battery cell assemblies can be seen in Figure 4. Several battery modules can also be structured strategically into battery packs so as to achieve even higher voltages, which is the case of a standard EV battery.

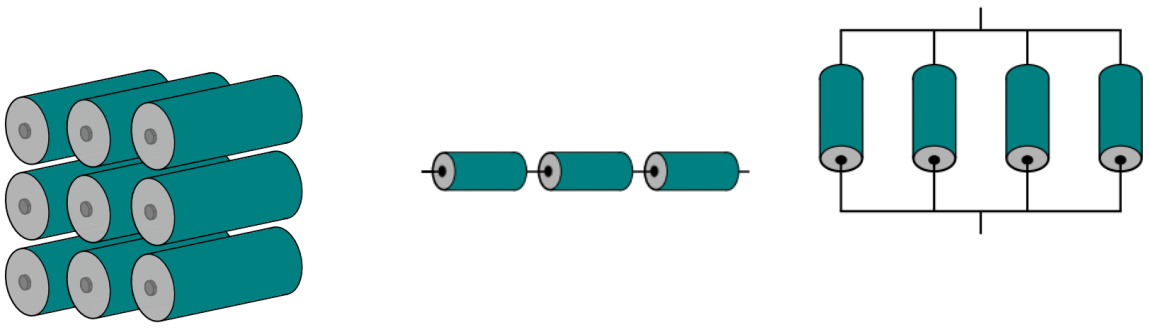

(a) Cells in a pack (b) Cells connected in series (c) Cells connected in parallel

Figure 4: Battery cell assemblies [20]

Safety concerns

High energy density is a sought-after characteristic in an EV battery, as mentioned previously. However, it has been demonstrated that materials with higher energy density come with lower thermal stability [22], usually leading into thermal runaway (TR). This phenomenon occurs when an initial rise in battery temperature triggers a cascading effect of further temperature increases. This can lead to significant hazards as it has the potential to escalate into malfunctions, and in the most severe instances, culminate in flammable danger such as battery fires and explosions.

Thus, it is always important to monitor battery safety, especially in batteries with automotive purposes such as EV batteries, which undergo intense use whenever a driving cycle is completed.

2.3.3 Battery Management System (BMS)

BMS refers to a management scheme that monitors, controls, and optimizes an individual battery performance or multiple battery modules in an energy storage system. [13]. The BMS is a crucial system control of the EV since it is responsible of safeguarding the battery by managing and ensuring a well functioning of the battery pack, thus avoiding potential hazards exposed in 2.3.2 to occur. To do so, it performs a set of various actions. The most relevant ones are: Monitoring, protecting and communicating the battery.

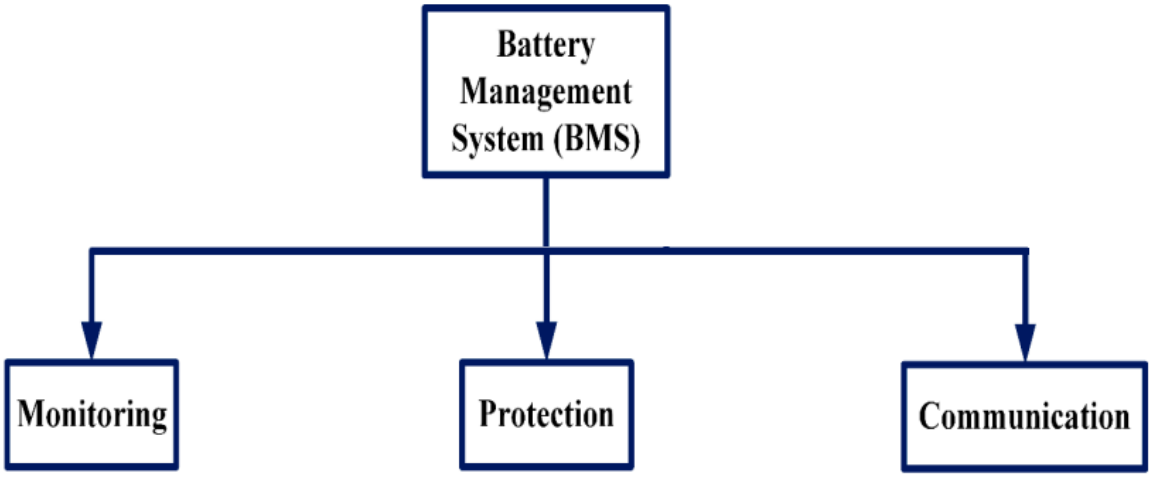

Figure 5: BMS functionalities. Adapted from [13]

Monitoring the state of battery

In order to take actions to ensure that the battery is performing under appropriate conditions, it is of vital importance to monitor the state of the battery pack and battery cells. This monitoring involves various characteristics, for example the total pack and cell voltage, the current, the health of individual cells, the state of balance of such cells, the temperature, etc. Along with the monitoring, computation is also performed. This consists in calculating and making estimations of other dimensions based on the previously monitored data. The most relevant estimations are the state of charge (SOC) and the state of health (SOH). They indicate the percentage level

of the maximum possible charge that is present inside a rechargeable battery, and the general condition of a battery along with its ability to deliver the specified performance in comparison with a fresh battery, respectively. [25]

It is of vital importance for the BMS and for the user to know accurately the SOC. The BMS will use this data to take proper actions to protect the battery, and the user will be able to know if the EV can be used and whether the battery needs to be recharged or not. Different estimation techniques exist for predicting the SOC. The principal state-of-the-art methods icnlude: Look Up Table (LUT) methods, Ampere-hour integral method (also known as Coulomb counting method), Filter-based methods, Observer-based methods and Data-driven based methods.

- LUT method: SOC estimated values are based on the mapping relationship between the the SOC value and characteristic battery parameters such as the IR, Open Circuit Voltage (OCV), etc. This method cannot be real-time implemented since the battery needs to be rested over an extended period of time so that the measured characteristic parameters are stabilized and accurate.

- Ampere-hour integral method: SOC estimated values are based on the integration of current flowing inside and outside the battery during a given time interval. It can be directly computed following the expression in Eq. 1 [23]:

$$SOC = SOC_0 + \frac{1}{C_N} \int_{t_0}^{t} I_{batt}\, dt \tag{1}$$

  where SOC_0 is a SOC starting point, C_N is the maximum battery capacity for a given SOH, and I_{batt} is the charging or discharging battery current. This method can be a source of accumulative errors if the initial SOC_0 is not well estimated. However, relatively easy solutions can be applied to solve this issue, such as the adaptive SOC reset time for estimating the OCV presented in [18].

- Filter-based methods: SOC estimated values are based on recursive processes that filter the input and output signals of the system to accurately predict the dynamic state of the system [21]. These methods are generally more robust and accurate but require higher computing resources and the accuracy of the SOC estimation is contingent upon the accuracy of the model.

- Observer-based methods: SOC estimated values are based on a state observer that can obtain estimated values of the state variables based on measured values of the system external variables. They can achieve satisfactory estimation accuracy but determining appropriate gain is still a pressing matter [32].

- Data-driven based methods: SOC estimated values are based on the idea that the internal dynamics of the battery are learned through considerable amounts of measurable input and output data. The most commonly used methods of this type include neural networks and fuzzy logic, among others. The main drawback of these methods are that they imply high computational cost and long processing time.

A quick and visual summary regarding different SOC estimation techniques has been included in Table 2.

Method	Representativeness	Accuracy	Application	Benefits	Drawbacks
• Look-up table method	❖ OCV look-up table method[46] ❖ Impedance look-up table method[53]	MAE≤±1.2% MAE≤±1.4%	Parked EVs, Lab Lab	√ Simple, easy to implement √ Simple, easy to implement, online	× Off-line, long relaxing time required × Sensitive to sensor accuracy
• Ampere-hour integral method	❖ Calculated by current integration[56]	MAE≤±4.0%	EVs, Lab	√ Simple, low computational cost	× Open-loop, rely on initial SOC and sensor accuracy
• Filter-based method	❖ Linear Kalman Filter (LKF)[60]	MAE≤±2.0%	EVs, Lab	√ Online, real-time	× Not suitable for nonlinear system
	❖ Extended Kalman Filter (EKF)[62]	MAE≤±1.4%	EVs, Implantable charger, Lab	√ Insensitive to uncertain initial state	× Depends on linearization error
	❖ Adaptive Extended Kalman Filter (AEKF)[75]	MAE≤±2.0%	EVs, Mobile robots, Lab	√ Robust to Gaussian noise	× Not suitable for non-Gaussian noise
	❖ Sigma-Point Kalman Filter (SPKF)[80]	ME≤±1.2%	EVs, Lab	√ No Jacobian matrix computation	× More computing resources required
	❖ Unscented Kalman Filter (UKF)[82]	ME≤±0.12%	EVs, Mobile robots, Lab	√ Suitable for high order nonlinear system, no Jacobian matrix required	× More computing resources Required, not suitable for non-Gaussian noise
	❖ Adaptive Unscented Kalman Filter (AUKF)[90]	ME≤±0.10%	EVs, Mobile robots, Lab	√ Robust to noise, high accuracy	× More computing resources required
	❖ Central Difference Kalman Filter (CDKF)[94]	MAE≤±1.42%	EVs, Spacecraft, Lab	√ No Jacobian matrix computation	× Limited to Gaussian noise
	❖ Cubature Kalman Filter (CKF)[96]	MAE≤±2.70%	EVs, Lab	√ Not limited to system type	× More computing resources required
	❖ Particle Filter (PF)[106]	MAE≤±0.863%	EVs, Lab	√ High accuracy, less computation time	× Need a complex mathematical tool
	❖ Unscented Particle Filter (UPF)[114]	MAE≤±0.9%	EVs, Lab	√ Better particle sampling	× Poor convergence rate
	❖ Cubature Particle Filter (CPF)[114]	MAE≤±1.1%	EVs, Lab	√ Better state probability approximation	× Poor convergence rate
• Observer-based method	❖ Luenberger Observer (LO)[118]	MAE≤±0.8794%	EVs, Lab	√ Fast convergence, high precision	× Difficult to determine observer gain
	❖ Sliding Mode Observer (SMO)[126]	ME≤±2%	EVs, Lab	√ Strong tracking, more stable	× Difficult to determine switching gain
	❖ PI Observer (PIO)[128]	ME≤±2.5%	EVs, Lab	√ Robust to sensor noise	× Difficult to determine PI gain
	❖ H-infinity/H_ Observer (HIO) [130]	ME≤±3.36%	EVs, Mobile robots, Lab	√ Robust to initial state	× More computing resources required
• Data-driven based method	❖ Neural Network (NN) method [141]	MAE≤±3.8%	EVs, Lab	√ Independent of battery model	× Dependent on training samples
	❖ Fuzzy Logic method[150]	ME≤±5.0%	EVs, Lab	√ Robust to operating conditions	× More computing resources required
	❖ Genetic Algorithm (GA)[33]	MAE≤±2.98%	EVs, Lab	√ Robust to system noise	× Complex calculation, slow response
	❖ Support Vector Machine (SVM)[156]	ME≤±6.0%	EVs, Lab	√ Better performs in nonlinear system	× More computing resources required

(Lab: Laboratory; EVs: Electrical vehicles; ME :Maximum error; MAE: Maximum absolute error)

Table 2: Comparison of different SOC estimation approaches [32]

On the other hand, the SOH is defined mathematically as in Eq. 2

$$SOH = \frac{Q_{max}}{Q_{new}} \tag{2}$$

where Q_{max} corresponds to the maximum available capacity of the battery, and Q_{new} is the available capacity of a brand new battery [32]. A way of estimating such available capacities generally involves counting full charge/discharge cycles, but as mentioned in [25], user usage of the battery also has great impact on this cycle-counting since it is generally uncommon to wait until a battery reaches full or empty battery capacity. Thus, adaptive systems that ensure an accurate SOC such as the ones mentioned previously can greatly contribute in obtaining a good and accurate SOH estimation.

Protecting the battery

Once the BMS has the necessary information, it takes action to ensure that the battery is kept within its safe operating region.

The unsafe operating mode may involve different abnormal conditions that could lead to catastrophic consequences. A summary of the principal hazards and their effects is provided along with the common BMS responses to protect the battery. [13, 14]

- Over-charging the battery cell: It consists in continuously charging a cell after it has already reached its full capacity state, thus provoking over-current. When over-charging takes place, physical composition battery cells can be destroyed, thus causing permanent damage to the battery and decreasing its lifespan. The BMS reaction to the over-charging phenomena is to turn off internal switches whenever the 100% SOC has been achieved, so that the battery cannot be further charged.

- Over-discharging the battery cell: Similar to the over-charging case but when discharging is taking place and 0% SOC has been achieved.

- Over-heating: This generally happens during discharging phase and essentially implies that the battery is at unsafely high temperatures. The BMS reaction to the over-heating phenomena is to control the environment by managing battery cooling systems (BCS) that will eventually lower battery temperature. BCS make use of fans and liquid coolant such as ethylene glycol in order to achieve their aim.

- Under-heating: It occurs when the battery is operating at too low temperatures, generally due to ambient temperature. The BMS reaction to the under-heating phenomena is to activate heating systems that will bring the battery back to normal operating temperatures.

- Over-voltage: It is a concerning hazard since it could lead to thermal runway. It is generally due to incorrect system design, use of incorrect charger or a consequence of overcharging the battery. The BMS reaction to the over-voltage phenomena is to set voltage back within safe operating limits by turning off switches that will prevent the battery from charging.

- Under-voltage: A minor loss in capacity and an increase in the self-discharge rate will occur. Whenever under-voltage takes place, it implies that the battery voltage is too low, resulting in a slow response when the starter starts. After prolonged usage, the dump wheel and the starter switch will suffer from damage. Additionally, long-term low voltage can shorten the life of the battery itself. The BMS reaction to the under-voltage phenomena is to set higher voltage to the battery pack unilaterally, disregarding the external inputs that are causing such phenomena.

The action taken can be of different types depending on the unsafe phenomena as previously seen. In general, the BMS will require external devices to reduce the charging or discharging magnitude of the battery, which can eventually lead to a reduction in the power released by the battery. Depending on the extent of this limitation, it might become noticeable to the driver. In extreme situations, it may be necessary to activate or deactivate internal switches, which could result in an open-circuit mode if the battery operates outside the safe operating area. As a consequence, this could completely disable the EV.

Finally, an EV battery involves multiple cells that could individually suffer from each of the already mentioned hazards. For practical purposes, the BMS is also in charge of the cell balancing process, which consist in setting all battery cells to same voltage levels or SOC. This allows to ensure that all cells are behaving in a similar way and thus the overall battery capacity can be maximized.

Communication of the battery

Of course in order to do the monitoring and protecting of the battery it is necessary to keep the central controller of the BMS communicated internally with its hardware operating at a cell level, or externally with high level hardware. Communication methods may be of several types also, such as serial communications, controller area network (CAN) bus or wireless communications.

3 Methodology

3.1 Battery model

As seen in 2.3.2, batteries are a complex structure. However, in order to study their overall behaviour, equivalent circuit models (ECM) can be conveniently used. An ECM uses electrical-circuit analogs to define a behavioral approximation to how a cell's voltage responds to different input-current stimuli [24], and the ECM components are capable of describing some crucial internal processes occuring inside battery cells.

There exist various types of ECM for batteries depending on the accuracy level that one is aimed to achieve. The simplest battery ECM is the one in Figure 6, where the battery cell is represented directly as an ideal voltage source that instantly provides constant voltage between its terminals. This voltage source is denoted as V_{OC} since it is of same magnitude as the open circuit voltage.

Figure 6: Ideal voltage source ECM. Adapted from [28]

Although this representation may be convenient under some circumstances, it is rather poor to deeply study battery behaviour. It has been seen from 2.3.3 that the SOH is an important parameter which indicates that battery degrades over time, and SOC levels also affects on battery performance. Therefore, it is precise to make use of less simplistic models.

A common way to represent the fact that a battery cell is degraded and not able to develop full voltage due to its level of SOH lower than 100%, is by adding a resistor to the ECM. This allows representing the phenomena that the voltage at the battery cell terminals (V_{cell}) is always lower than the V_{OC} whenever the circuit is charging, and higher when it is discharging [24]. The resistor is denoted as R_{int}, and essentially represents the IR of the battery cell.

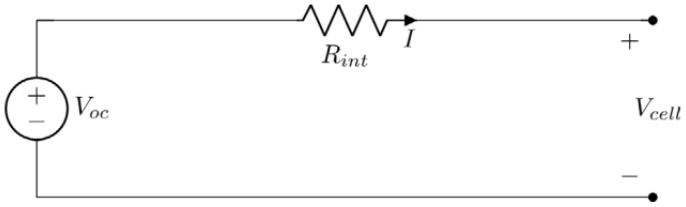

Figure 7: Series resistance ECM. Adapted from [28]

The equivalent series resistance model is generally enough for simple electronic-circuit designs, but not for the large scale case of EV batteries. Within this context, it is common to observe that the movement of electrons between the anode and the cathode of the cell create a difference

in ion concentrations and result in diffusion or polarization voltages. These are defined as the change of cell voltage from its open-circuit voltage that appear during the charge and discharge states [27]. In [24], it is presented the voltage response during a discharge pulse of 15 min of duration. Afterwards, the battery is disconnected from the load and it can be clearly seen that the voltage response starts to slowly evolve in time until finally reaching steady state.

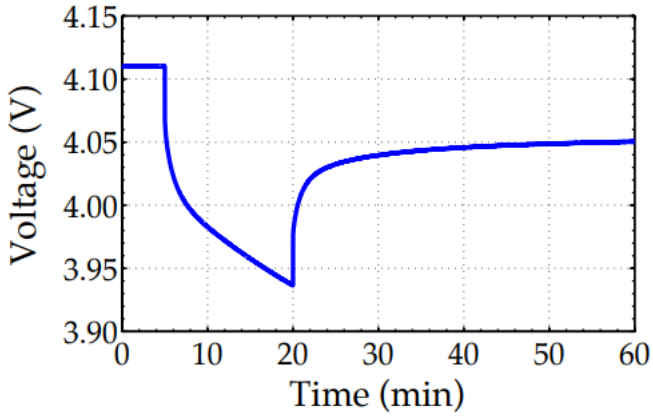

Figure 8: Response to discharge pulse [24]

In literature, it is very common to see batteries represented as a Randle circuit model of various orders in order to depict accurately the phenomena presented in Figure 8. This ECM is represented as a simple circuit consisting of the already seen V_{OC}, and R_{int} in series with n-RC branches of a resistor and a capacitor in parallel. The number of RC branches depends on the accuracy desired to be obtained. More precise results are obtained with higher n. Nonetheless, if n increases, so does complexity and more computational resources are needed.

The most commonly used ECM include at most up to 3-RC branches. From [30], it is obtained that the 2-RC model shown in Figure 9 is optimal, since it is simple and computationally light while at the same time it represents the dynamic behaviour of a cell with good accuracy. Consequently, this is the model that will be used to achieve the thesis objectives of study.

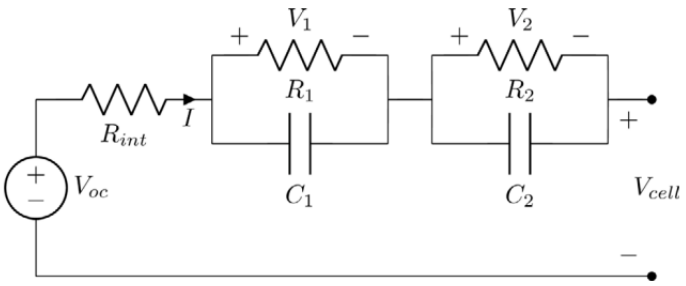

Figure 9: R-2RC ECM [28]

The parameter values of the R-2RC model are highly dependent on the charging/discharging mode, the SOC, and the SOH of the battery cell. Further real-life accuracy can be achieved by also considering temperature at which the battery is operating.

$$V_{OC} = f(SOC, SOH, T) \tag{3}$$
$$R_{int} = f(SOC, SOH, T) \tag{4}$$
$$R_1 = f(SOC, SOH, T) \tag{5}$$
$$C_1 = f(SOC, SOH, T) \tag{6}$$
$$R_2 = f(SOC, SOH, T) \tag{7}$$
$$C_2 = f(SOC, SOH, T) \tag{8}$$

These parameters can be determined experimentally. It is very common to store such results in LUT which can later be used to study the behaviour of the cell at given SOC and SOH levels. In *Open data model parameterization of a second life Li-ion battery* [28], parameter values are given for SOC values from 0% to 100% of Li-ion batteries with a SOH from 50% to 80%.

The Li-ion battery used for the so mentioned study has characteristics exposed in Table 3 .

Cell format	18 650
Positive electrode	NMC + LMO
Specific capacity	158.5 mAh g^{-1}
Negative electrode	Graphite
Specific capacity	309 mAh g^{-1}
Cell capacity	2.1 Ah
Max. charge rate	1C
Max. discharge current	−10 A
Operating temperature	0 °C–45 °C

Table 3: Investigated cell characteristics [28]

The nominal cell capacity parameter ($C_{N,c} = 2.1Ah$) provided by Table 3 is highly relevant for this thesis. Moreover, from [24] it is obtained that majority of Li-ion cells operate at a nominal voltage of around 3.7 V ($V_{N,c} = 3.7V$). In Section 3.5, usage of this magnitudes will be required.

R-2RC dynamics

In order to study the battery behaviour, it is needed to know its dynamics over time. The particularity of this ECM is that its V_{cell} at a given instant of time will not only depend on the current at that time, but also on past current magnitudes due to the RC branches and their capacitance effect. If the current flowing through R_{int}, R_1 and R_2 at time t is denoted as $i_{cell}(t)$, $i_1(t)$ and $i_2(t)$ respectively, then the ECM V_{cell} can be modelled in terms of $i_{cell}(t)$ by Eq. 9 to 11 [24]:

$$i_1(t) = \exp\left(-\frac{dt}{R_1 \cdot C_1}\right) \cdot i_1(t-1) - \left(1 + \exp\left(-\frac{dt}{R_1 \cdot C_1}\right)\right) \cdot i_{cell}(t) \tag{9}$$

$$i_2(t) = \exp\left(-\frac{dt}{R_2 \cdot C_2}\right) \cdot i_2(t-1) - \left(1 + \exp\left(-\frac{dt}{R_2 \cdot C_2}\right)\right) \cdot i_{cell}(t) \tag{10}$$

$$V_{cell}(t) = V_{OC} + R_{int} \cdot i_{cell}(t) - R_1 \cdot i_1(t) - R_2 \cdot i_2(t) \tag{11}$$

It is important to remark that all expressions in this thesis follow the same current sign convention where $i_{cell}(t) < 0$ for a discharging current, and $i_{cell}(t) > 0$ for a charging current.

Parameters extension

This thesis uses data provided in [28]. Moreover, additional values of SOC and SOH have been interpolated and extrapolated respectively. By doing so, it has been possible to extend the LUT and include values of parameters for the case of 90%-100% SOH, and for levels of SOC up to 2 decimal numbers.

The advantageous part of this LUT extension is that simulations are capable to be more accurate in the sense that during a driving cycle, the battery SOC can vary very little and the original LUT may not be able to capture all these small SOC changes. For instance, the original LUT considers values of 50% SOC and the next level given is 70% SOC. Thus, a range of 20% of SOC that is very likely to be needed in some simulations is directly missed. Furthermore, the extrapolation up to 100% SOH is convenient since comparisons between a brand new battery and a degraded one with lower SOH can be made.

SOH extrapolation

It is found in literature that R_{int} follows an inversely proportional trend with SOH levels [16,19, 27]. However, R1, C1, R2, C2 and V_{OC} do not follow any particular predefined trend. In front of this lack of information, all parameters are extrapolated for a level of 100% SOH following a least squares polynomial fit of 1^{st} order degree. This polynomial regression is mathematically valid, but at some points it yields results that do not have any physical meaning, such as negative values. In order to make sure that no non-sense results are obtained, an assumption is made and a constraint is set: whenever a negative value is obtained, the parameter magnitude for 100% SOH is set to be the same one as for 80% SOH.

The initial LUTs give parameter values depending on SOC and SOH, and different LUTs are used for different temperatures. Therefore, a single extrapolation for 100% SOH was made keeping constant the SOC, and this process was repeated for all available data SOC levels.

A visual inspection for all SOC percentages was made by plotting the extrapolated point of 100% SOH (orange) along with the rest of given SOH levels (blue). A sample of some of the obtained plots at SOC=[0, 50, 80, 100] % for the particular case of R_{int} at charging mode and at 25 ºC can be seen in Figures 10a, 10b, 10c and 10d.

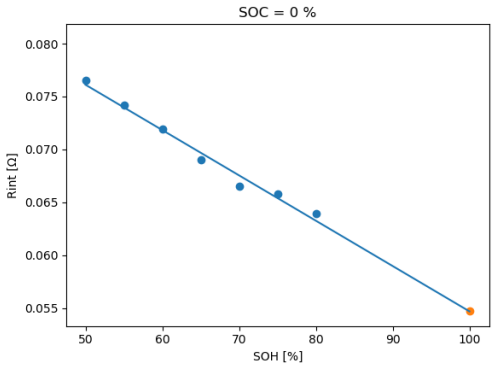

(a) R_{int} at SOH=[50-100]% and SOC=0%

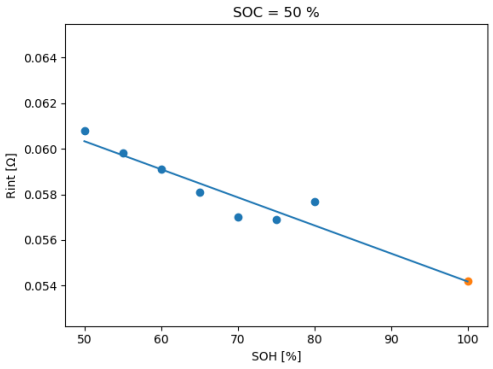

(b) R_{int} at SOH=[50-100]% and SOC=50%

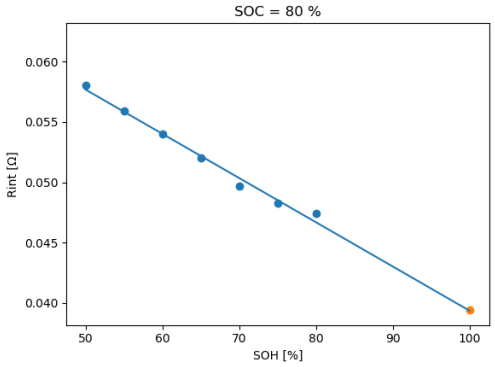

(c) R_{int} at SOH=[50-100]% and SOC=80%

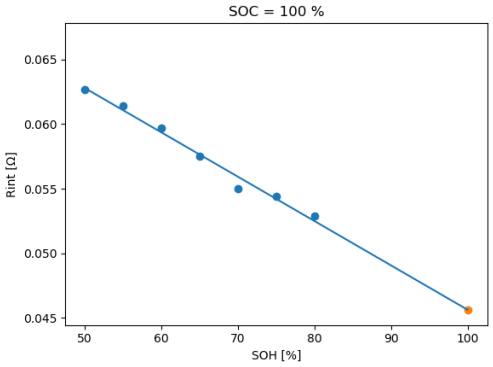

(d) R_{int} at SOH=[50-100]% and SOC=100%

Figure 10: R_{int} extrapolation at SOH=100% for certain SOC levels

Additionally, the resulting 100% SOH points were all plotted together to see its overall trend and compare it with the rest. In Figure 11, the R_{int} trend depending on the SOC at a level of SOH=100% is depicted in red, while the other blue trends represent the remaining original LUT values for R_{int}.

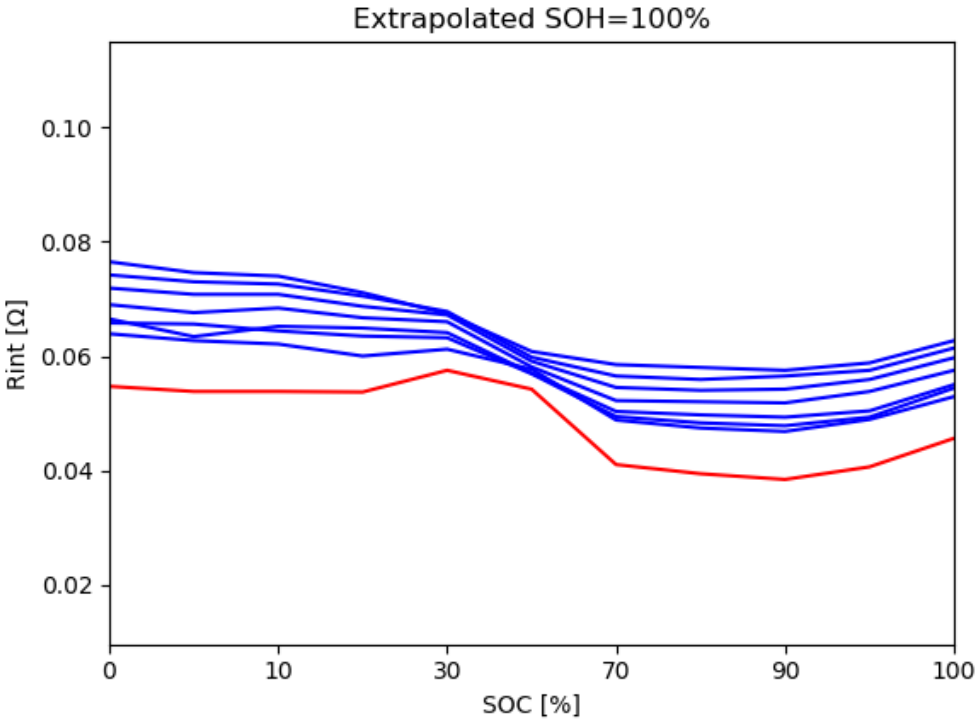

Figure 11: Extrapolation of R_{int} at a SOH=100% for all values of SOC

SOC interpolation

Finally, the parameters were interpolated so as to obtain additional SOH magnitudes between 50% and 100% with a step of 1%, and for SOC between 0% to 100% with a step of 0.01%. In Figure 12, interpolated trends for SOH=[80,100]% can be seen in cyan colour, while blue trends are for the interpolations of data provided and the red trend shows the parameter values at a SOH=100% as in Figure 11.

The described process has been applied to all LUTs found in [28]. The entire used code is included in Annexes B.1.

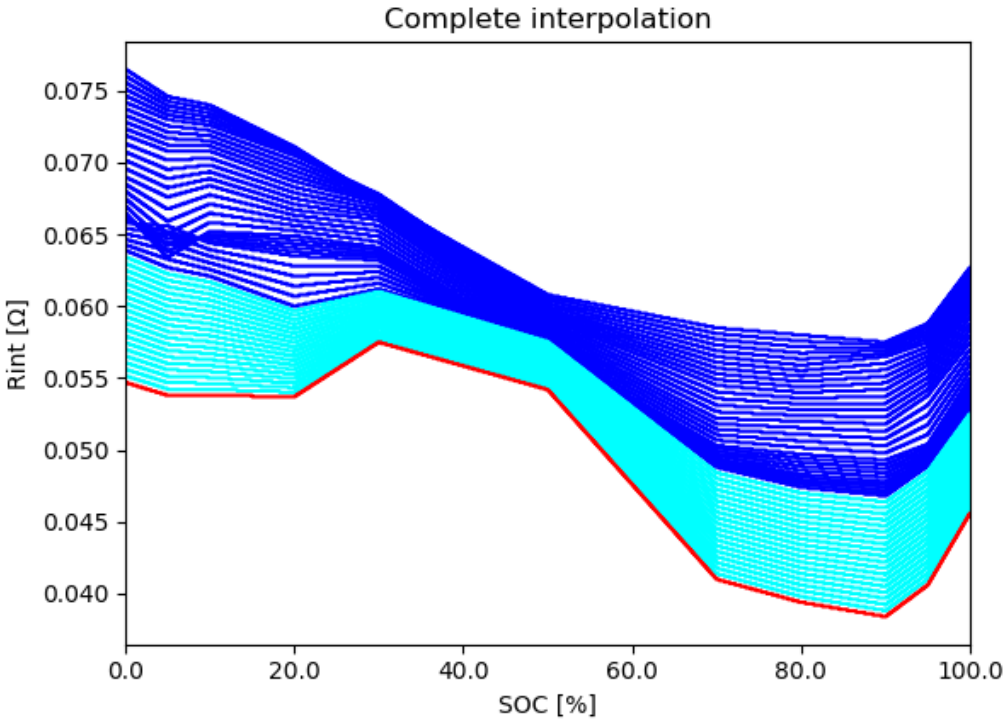

Figure 12: R_{int} interpolation at more detailed levels of SOH and SOC

3.2 Road vehicle dynamics

The vehicle has been modelled taking into account the dynamics that may occur during a real life driving cycle. As presented in [20], all gravitational force (F_g), traction force(F_t), aerodynamic drag (F_a) and rolling resistance (F_r) must be taken into account. A scheme depicting all forces acting on a road vehicle in motion can be seen in Figure 13.

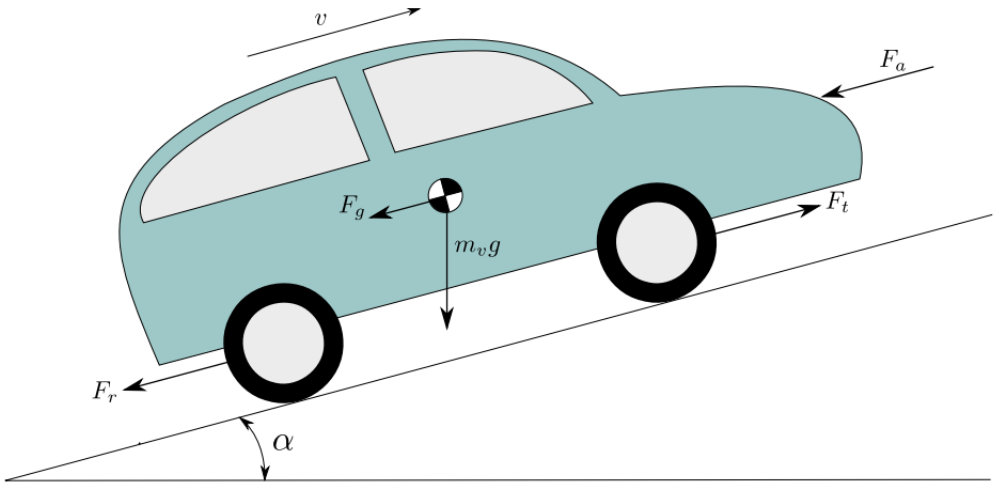

Figure 13: Forces acting on a road vehicle in motion [20]

Aerodynamic drag ($\mathbf{F_a}$)

Aerodynamic drag is, by definition, the force that opposes to the relative motion of an object through the air. It is of great importance in the automotive field, specially when the car is travelling at high speeds. This force depends on the frontal section of the vehicle (A_f), the air density (ρ_a), the aerodynamic drag coefficient (c_d) and the velocity at which the car is travelling (v). Its general expression is seen in Eq. 12.

$$F_a = \frac{1}{2} \cdot \rho_a \cdot A_f \cdot c_d \cdot v^2 \tag{12}$$

Gravitational force ($\mathbf{F_g}$)

The gravitational force appears whenever the vehicle is circulating in a sloped road. It will act as a force opposing to motion if slope is positive or negative. This will mean that the car is going uphill or downhill, respectively. In cases where the road is flat, the gravitational force will only act in the direction of gravity, and therefore it will not contribute nor oppose to the motion of the vehicle. The general expression for this force is exposed in Eq. 13.

$$F_g = m_v \cdot g \cdot sin(\alpha) \tag{13}$$

where m_v is the mass vehicle, g is the gravity and α corresponds to the slope of the road.

Rolling resistance ($\mathbf{F_r}$)

This force appears when a body rolls on a surface, such as the vehicle tires on the road. It opposes to motion, and it can have huge impact on vehicle performance. Some studies have reached the conclusion that ICE devote around 5 to 15% of the fuel energy exclusively to overcome rolling resistance in regular passenger vehicles [17]. Thus, they greatly impact on all types of road vehicles, such as EVs. This force is computed according to Eq. 14.

$$F_r = c_r \cdot m_v \cdot g \cdot cos(\alpha) \tag{14}$$

where c_r is the rolling resistance coefficient, a parameter that depends on the tire material and on the road surface.

Traction force ($\mathbf{F_t}$)

Traction force is the force that is needed to overcome resistance and move a vehicle along the road. It does not have any predefined general expression since it depends on the particular dynamics of the body and the environment surrounding it. However, traction force can be computed with expression seen in Eq. 15, obtained by using Newton's second law of motion.

$$F_t - F_a - F_g - F_r = m_v \cdot a = m_v \cdot \frac{d\, v(t)}{dt} \tag{15}$$

In this expression, the term a refers to the linear acceleration of the vehicle, which is defined as the derivative of the velocity.

3.3 Connection between vehicle dynamics and battery model

Now, it is of vital importance to determine how the battery behaviour interacts with the road vehicle dynamics. In an EVs, all traction force of the car is given only by the electric battery (P_b). Thus, the power delivered by the battery is closely related to the traction power (P_t).

The traction power of a car is obtained from velocity (v) and traction force as presented in Eq. 16. Now assuming that all traction force comes from the power consumption of the battery, and that the power electronics and the electric motor have an efficiency of η_{em} and η_{pe} (they are not considered as ideal), then Eq. 17 is obtained.

$$P_t = F_t \cdot v \tag{16}$$

$$P_b = -P_t \cdot (\eta_{em} \cdot \eta_{pe})^{-(sgn(P_t))} \tag{17}$$

with sgn being defined as the signum function.

Additionally it is known that the electric power is defined as in Eq. 18 as the battery voltage times the battery current.

$$P_b = V_b \cdot I_b \tag{18}$$

Therefore, by combining Eq. 12 to 18, expression in Eq. 19 can be achieved.

$$I_b = \frac{(m_v \frac{d\ v(t)}{dt} + c_r m_v g cos(\alpha) + m_v g sin(\alpha) + \frac{1}{2}\rho_a A_f c_d v^2) \cdot v}{V_b} \cdot (\eta_{em} \cdot \eta_{pe})^{-(sgn(P_t))} \tag{19}$$

Moreover, the battery voltage depends on the battery configuration and the total number of cells available in the overall battery. If s is the number of cells that are arranged in series, and p is the number of cells that are arranged in parallel, then the total battery voltage and current can be computed according to Eq. 20 and 21.

$$V_b = V_{cell} \cdot s \tag{20}$$

$$I_b = i_{cell} \cdot p \tag{21}$$

Finally, if Eqs. 11, 19 , 20 and 21 are combined, the cell current i_{cell} required for moving the car at a desired velocity v can be derived in terms of the battery parameters and vehicle characteristics as the expression in Eq. 22.

$$i_{cell} = \frac{(m_v \frac{d\ v(t)}{dt} + c_r m_v g cos(\alpha) + m_v g sin(\alpha) + \frac{1}{2}\rho_a A_f c_d v^2) \cdot v}{(V_{OC} + R_{int} \cdot i_{cell} - R_1 \cdot i_1 - R_2 \cdot i_2) \cdot s \cdot p} \cdot (\eta_{em} \cdot \eta_{pe})^{-(sgn(P_t))} \tag{22}$$

3.4 Driving cycles

Driving cycles aim to simulate real-world speed driving scenarios for a particular geographical area and time period. They are standardized test procedures used to evaluate vehicle performances relative to various aspects such as vehicle emissions, fuel consumption, etc. Many types of driving cycles exist, and their characteristics depend greatly on the aspect to be determined [1,11].

The most common way to classify driving cycles is by the area they are simulating:

- Urban Driving Cycles (UDC): They simulate urban areas. The speed does not reach high values and there are multiple accelerations and decelerations so as to recreate stops due to traffic lights, pedestrians, etc. The duration is also generally slower.

  Some common Urban driving cycles include the Artemis Urban and the Federal Test Procedure - 75 (FTP-75).

- Highway/Motorway Driving Cycles (HDC): They simulate driving in highways. The speed reaches high values during prolonged amounts of time and it generally only reaches to a value of zero at the beginning and at the end of the driving cycle.

  Some common Highway driving cycles include the Artemis Mw130, Artemis Mw150, and the Highway Fuel Economy Test (HFET).

- Combined Cycles: They simulate a combination of urban and highway driving cycle.

  Some common Combined cycles include the Artemis Rural Road, the New European Driving Cycle (NEDC) and the World Harmonized Light Vehicles Test Procedure (WLTP).

- Real Cycles: Other driving cycles also exist, such as Real-world Driving cycles which obtain simulations from real-world data driving parameters.

In this thesis it is primarily used the Artemis cycles, both urban, motorway (Mw) and combined varieties. These correspond to the Urban, Motorway 130 (and the Motorway 150) and the Rural Road, respectively. Artemis is widely used in European projects, and the 4 different varieties simulating around 1080 seconds of driving cycle can be seen in Figures 14, 16 and 15.

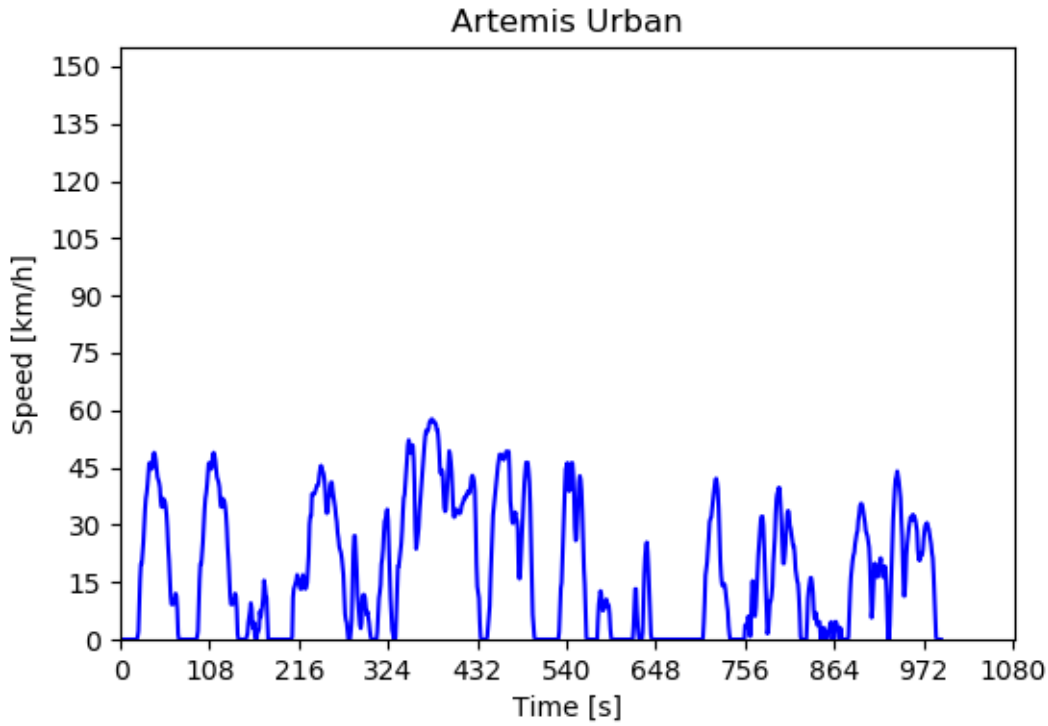

Figure 14: Artemis Urban Driving Cycle

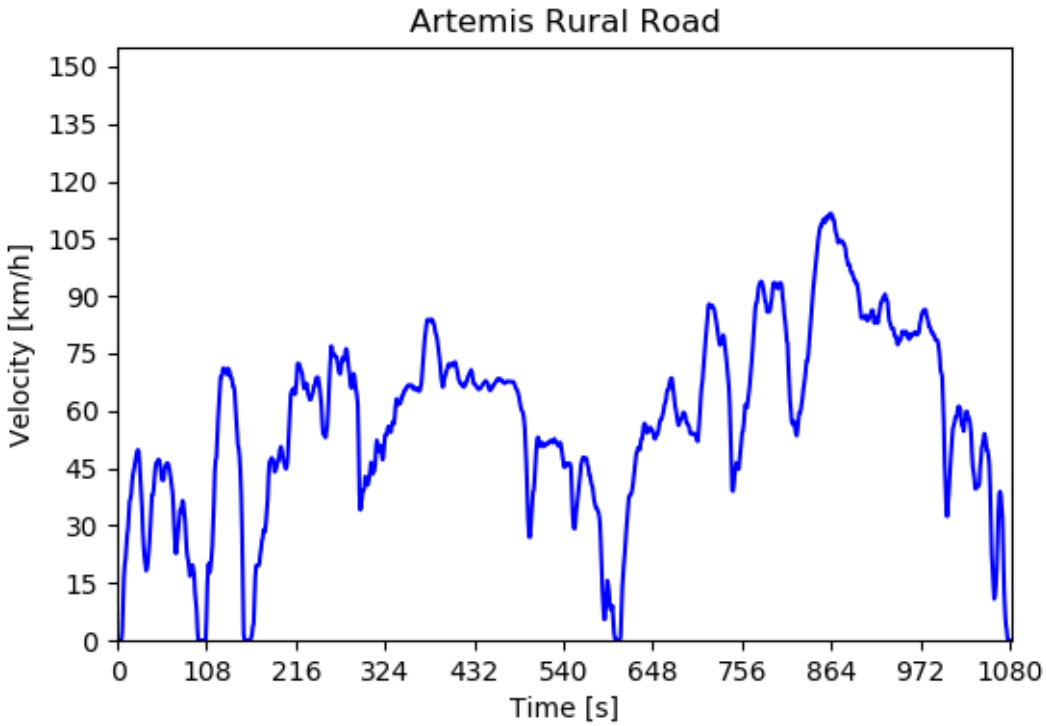

Figure 15: Artemis Rural Road Driving Cycle

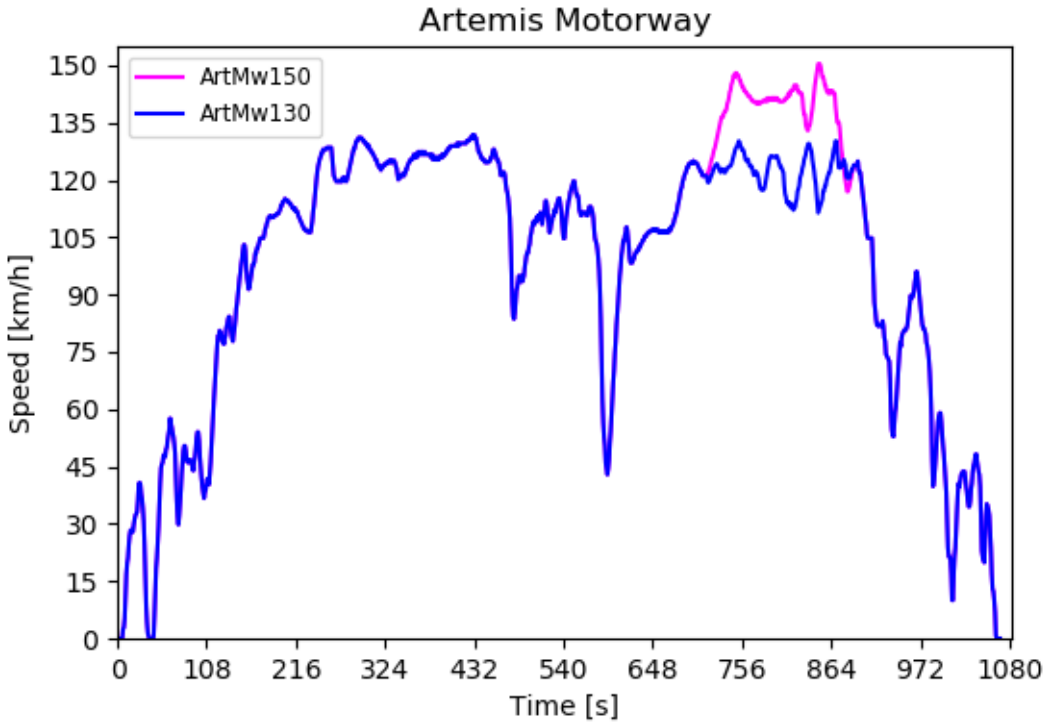

Figure 16: Artemis Motorway Driving Cycle

A real driving cycle is also used so as to see the differences between predetermined standard cycles and a real one. The speed driving profile can be seen in Figure 17.

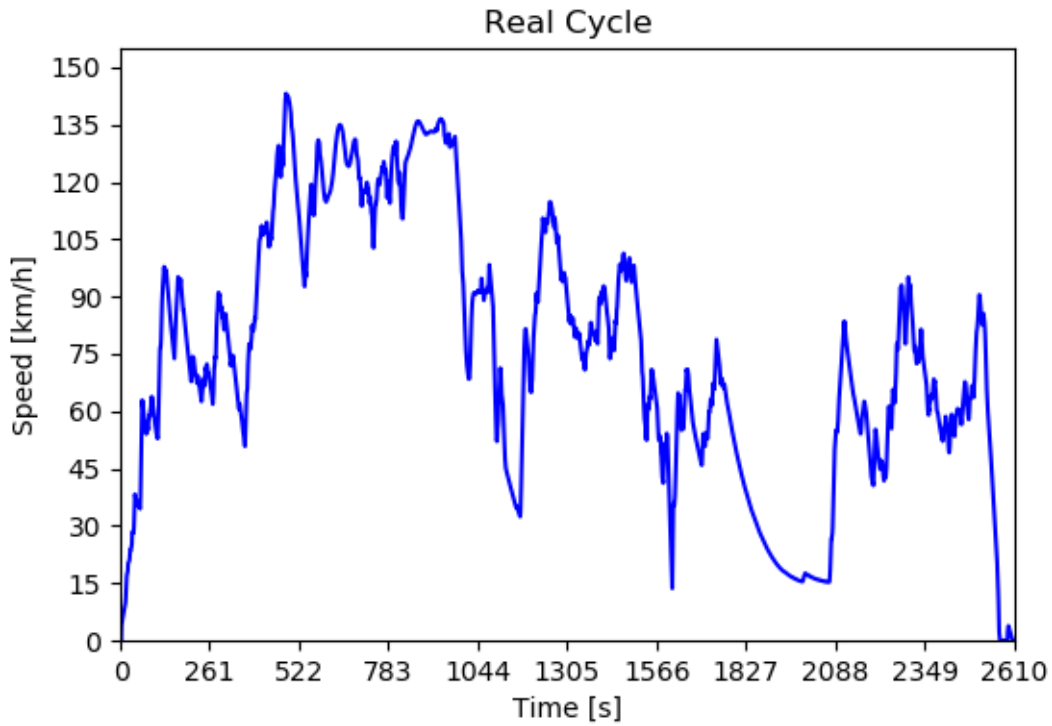

Figure 17: Real Driving Cycle

3.5 Vehicle model choice

It is important to characterize the dimensions of our car because of the impact that this will have on the vehicle dynamics. Many different type of cars exist. Some may be more aerodynamic than others and weight also varies between models. Nevertheless, it is arbitrarily decided to use model Citroën ë-C4 in this thesis for the main simulations with the Artemis driving cycles. This choice was made because its battery cells are made of Li-ion, which makes it suitable for the battery parameters that will be used. Moreover, its average position in price and battery characteristics with respect to the other EV in the market make it more accessible for all publics.

Figure 18: Citroën ë-C4 model

In Table 4, the most relevant parameters for the study of road vehicle dynamics are provided. Data such as the mass vehicle, the frontal area and the battery characteristics have been collected from EV Database. Additionally, characteristics not provided by the manufacturer nor by the so mentioned data base (such as the drag coefficient, rolling resistance coefficient or motor efficiencies) have been assumed to be of the same value as the ones presented in [20].

By assuming that the Li-ion battery of the Citroën ë-C4 model is made of multiple battery cells with characteristics exposed in Table 3, it can be obtained the battery configuration. Only 2 battery configurations exist: the parallel-serial and the serial-parallel. The parallel-serial configuration consists of parallel branches, each comprising multiple cells arranged in series. Conversely, the serial-parallel configuration follows the reverse arrangement, with series-connected cells grouped in parallel. Representations of these arrangements can be seen in Figure 19a and Figure 19b, respectively. Ideally, the voltage delivered by both assemblies should be the same. Thus, by taking the parallel-serial configuration as a reference and knowing the basics of electric circuits, the number of parallel (p) and series (s) cells can be computed as following:

$$p = \frac{P_{N,b}}{V_{N,b} \cdot C_{N,c}} = \frac{50\ 000\ Wh}{400\ V \cdot 2.1\ Ah} \approx 60 \tag{23}$$

$$s = \frac{V_{N,b}}{V_{N,c}} = \frac{400\ V}{3.7\ V} \approx 108 \tag{24}$$

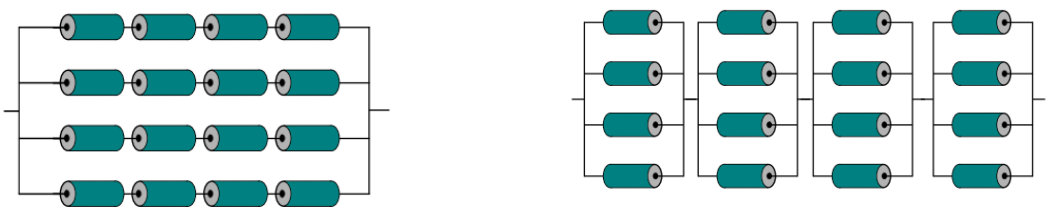

(a) Parallel-serial configuration (b) Serial-parallel configuration

Figure 19: Battery configuration types [20]

Parameter	Value	Unit	Description
ρ_a	1.2922	kg/m^3	Air density
A_f	2.745	m^2	Frontal section of the vehicle
c_d	0.3	-	Aerodynamic drag coefficient
m_v	2020	kg	Mass vehicle
g	9.82	m^2/s	Gravity
c_r	0.01	-	Rolling resistance coefficient
η_{em}	0.85	-	Electric motor efficiency
η_{pe}	0.95	-	Power electronics efficiency
$P_{N,b}$	50	kWh	Nominal battery capacity
$V_{N,b}$	400	V	Nominal battery voltage
$V_{N,c}$	3.7	V	Nominal cell voltage
$C_{N,c}$	2.1	Ah	Nominal cell capacity

Table 4: Citroën ë-C4 and road dynamic parameters

3.6 Assumptions and simplifications

Deep study of EV batteries requires computing effort, resources and time. In order to make this thesis more approachable, some key assumptions and simplifications were made. In the next lines, these will be explained.

Temperature disregard

For the sake of simplicity, temperature effects are disregarded and all simulations are assumed to be held at a constant temperature of 25 ºC, ignoring the heating of the battery during operation mode and thermal runway issues. In other words, it is pressumed that the temperature at which the battery is found is only determined by ambient temperature. This temperature is chosen because the open data parameters from [28] provide LUT only at 2 temperatures: low at 0 ºC and high at 25 ºC. Consequently, it is assumed that temperature does not have any impact on SOC levels of the battery nor on its ECM parameters.

Therefore, assuming that the simulations are conducted in Southern Europe during spring or fall seasons, it could be realistic to suppose that an ambient temperature of 25ºC can be ensured.

Acceleration computation

Artemis driving cycles provide speed values during a given time interval. From these, acceleration can be found.

2 main formulas to compute the acceleration at time t apply and are exposed in Eq. 25 and 26.

$$a(t) = v(t) - v(t-1) \tag{25}$$

$$a(t) = \frac{v(t+1) - v(t-1)}{2} \tag{26}$$

Eq. 25 is convenient whenever a straightforward measure is required. However, Eq. 26 is more suitable for cases in which a smoother estimation of the acceleration wants to be made. For easy computing purposes, the first option is chosen to obtain acceleration in all the simulations.

Cell balancing

Cell balancing is held by the BMS as a safety measure in real life, thus it is assumed to occur in the simulations too. Therefore, it is supposed that all cells have same SOH and SOC. These values also coincide with the overall battery SOH and SOC, and by computing these characteristics for a single cell, it is obtained the overall battery SOC and SOH.

Constant SOH

As seen in Section 3.4, the Artemis cycles have a duration of at most 1083 seconds, which corresponds to 18 minutes. Since this period is rather short, it is assumed that the SOH is kept at constant value along a full simulation. In reality, the SOH will decay, but the decrease that may ocurr during this 1083 seconds is assumed to be so small that in this thesis it is directly neglected. By doing so, computations can be further simplified.

SOC estimation

The Ampere-hour integral method is the one considered in this thesis as it is the most commonly used technique for the SOC estimation in practice [23]. As stated in Section 2.3.3, the SOC is defined by Eq. 1. Moreover, the SOC needs to be within the range of 0% to 100%. Whenever the SOC reaches a value of 0%, all simulations are stopped as it is considered that the battery is no longer able to provide any electricity.

Constant slope

There exist some studies such as [29] that model slope cycles from speed driving cycles. Nevertheless, in this thesis it is assumed constant slope along the whole driving cycle for simplicity purposes. In order to obtain more varied results, cases for α=0º and for α=5º are both simulated. The 5º choice is due to the intention of modelling an average steep road that is within correct range to assume it generalizable and realistic enough.

Regenerative braking

Regenerative braking is a very useful mechanism that allows charging the battery of the EV during the driving cycle at deceleration moments. It is the term that represents the conversion of kinetic energy from the wheels into electrical energy to the battery, and it is a form of optimizing vehicle's performance and not waste energy. Nowadays, all vehicles have regenerative braking, and it ultimately implies that whenever the current of the battery is positive ($I_b > 0$), the SOC will increase thanks to the cell battery 'charging mode'.

BMS actions

In this thesis, focus is driven to voltage management from the BMS, especially on the undervoltage control due to the purpose of studying how the battery degradation can affect on driving. This occurs whenever the voltage required is below the safety values, so that voltage is then imposed by the BMS and power delivered by the battery lowers, thus not being able to reach

desired velocities.

The threshold set to reaching undervoltage is set at 2.8 V per each cell, following state of the art voltage limits for Li-ion batteries [3,7,15]. Additionally, the cell overvoltage limit is determined by [28] at 4.2 V, so upper voltage limits are also implemented, although these don't have any direct effect in driving.

Knowing that the battery is composed by 108 cells in series, it can be obtained that the overall battery operational lower and upper voltage limits correspond to 302.4 V and 453.6 V, respectively.

3.7 Summary of the simulation

The simulation consists in obtaining a target current profile that the car needs to fulfill in order to achieve desired speed profile defined by a certain driving cycle, by using the expression defined in Eq. 22. To solve this expression, the battery parameters at a given initial SOH and SOC are given, along with road and vehicle parameters such as the slope or the car dimensions.

A voltage profile is then obtained from the current profile by using Eq. 11, and the BMS will keep the reading of these values. In case of working under safe operating conditions, the BMS will not intervene at any point. Nevertheless, if the battery is working at undervoltage, the BMS will intervene by setting appropriate voltage levels, and current will be recalculated according to the minimum allowed voltage using Eq. 11 again. However, if the battery is working at overvoltage, the BMS will act by setting appropriate voltage but current will remain the same.

Under the recalculation case when undervoltage is occurring, a new resulting current profile is defined. Finally, the current profile will be used to obtain final resulting velocities, taking into account again the battery and vehicle model.

A diagram showing the process in a summarized way can be seen in Figure 20, and the entire used code is included in Annexes B.2. Notice that when there is no undervoltage, the resulting current profile will be the same as the target current profile, thus the resulting driving cycle speed profile will be also the same as the desired driving cycle speed profile.

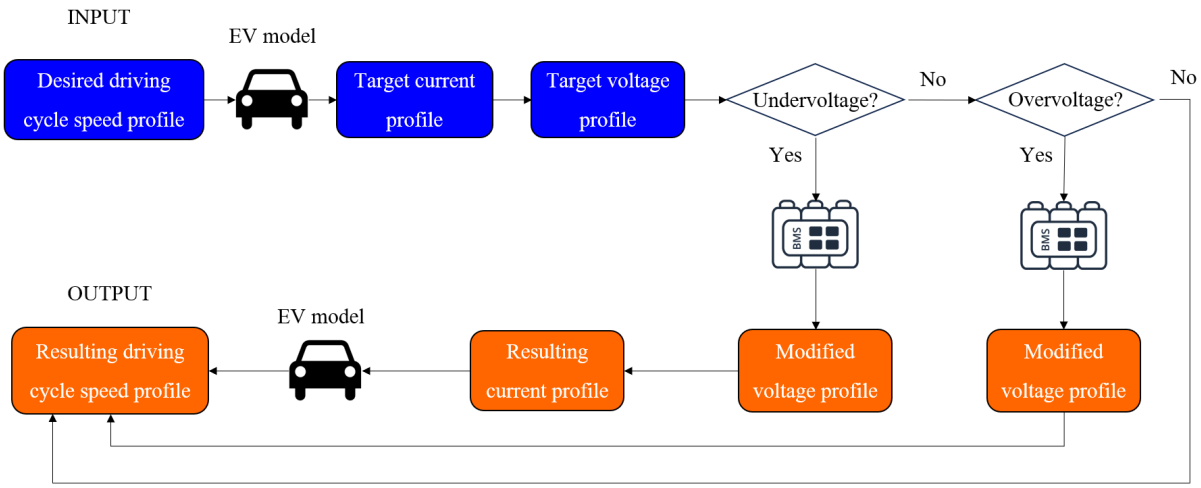

Figure 20: Summarized process diagram

4 Results

In the following section, results for the carried simulations are presented. For each simulation at a given initial SOH, SOC and slope (α), 4 graphs are exposed corresponding to the voltage profile (a), the power profile (b), the speed profile (c) and the SOC profile (d) during the specified driving cycle. Target profiles are represented in black color for each figure in order to visually see the differences between the profiles if the BMS did not intervene versus if it does.

4.1 Artemis Urban driving cycle

Simulations for the Artemis Urban driving cycle are exposed in this section. This driving cycle is the least demanding one. Maximum speed is significantly lower and multiple accelerating and decelerating occur.

SOH = 50%, SOC = 30%, α = 0º

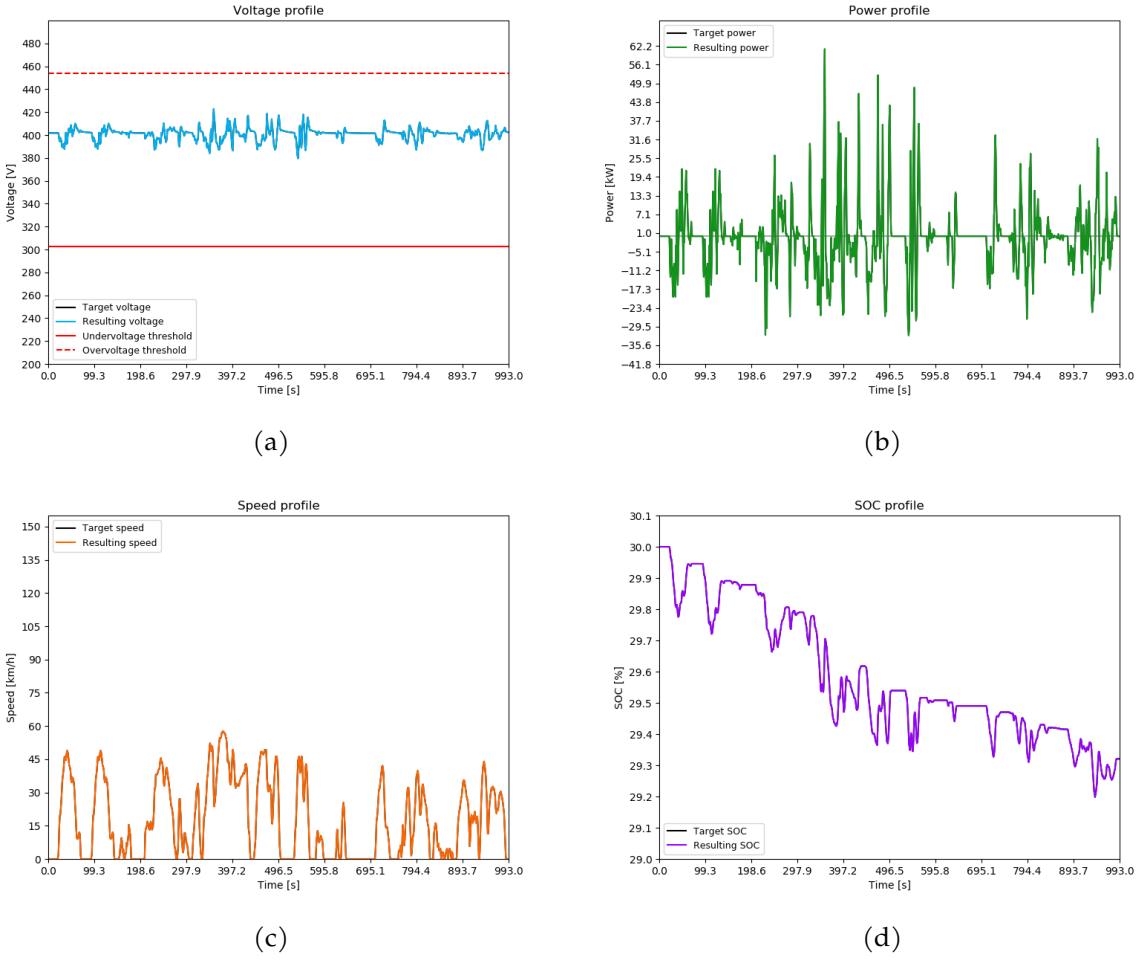

(a) (b)

(c) (d)

Figure 21: ArtUrban at SOH=50%, SOC=30%, α=0º

It can be observed that target profiles are not seen. This means that the target and the resulting profiles coincide since the BMS intervention was not required because voltage is within correct

operational limits at all times of the simulation. Thus, for a low SOH, low SOC and a plain road, the EV is found to be capable of finishing the simulation properly. Additionally, the SOC decrease is of 0.68% thanks to the multiple deceleration which allow to periodically recharge the battery due to regenerative braking. This implies that the EV model would actually be capable of successfully completing the same driving cycle a few more times.

SOH = 50%, SOC = 30%, α = 5º

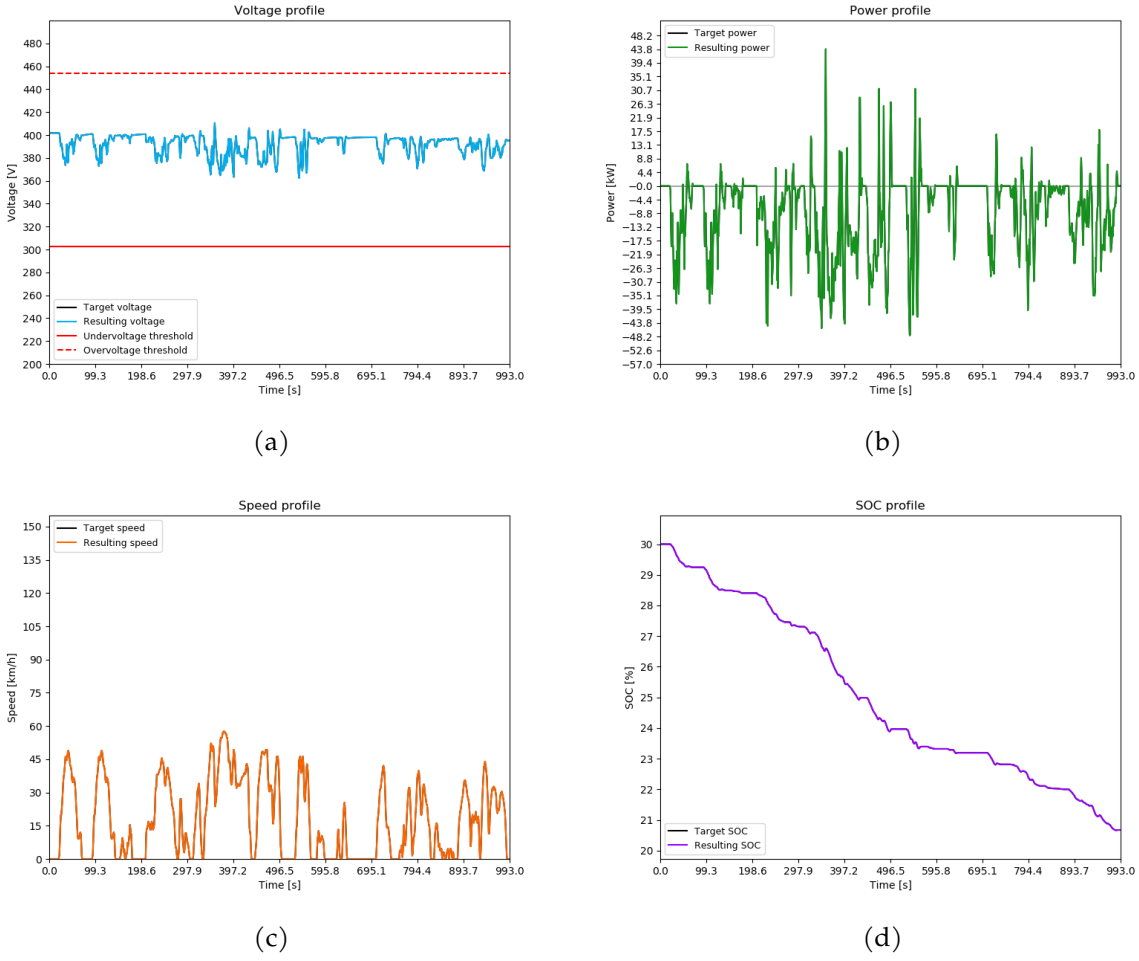

Figure 22: ArtUrban at SOH=50%, SOC=30%, α=5º

Only the road conditions have been modified with respect to the simulation presented in Figure 21 and now, where α=5º. Despite the fact that the driving cycle is now more demanding, it can be observed that the vehicle is also capable of finishing properly the simulation without intervention of the BMS. It is interesting to observe that now the SOC decreases around a 9.32% due to this change in road slope and an increase in the required traction power.

Simulations for the cases of better SOH and SOC conditions were held, and all of them resulted in lack of undervoltage nor appreciable overvoltage and enough initial SOC to terminate the driving cycle. Summary of the simulation results for different initial parameters is presented in

Table 5.

Driving cycle	SOH (%)	SOC (%)	Alpha (º)	Voltage Modified	Cause	Enough SOC	SOC Loss (%)
ArtUrban	100	100	5	NO	-	YES	-4.02
ArtUrban	100	80	5	NO	-	YES	-4.23
ArtUrban	100	60	5	NO	-	YES	-4.53
ArtUrban	100	50	5	NO	-	YES	-4.69
ArtUrban	100	30	5	NO	-	YES	-4.79
ArtUrban	80	100	5	NO	-	YES	-5.06
ArtUrban	80	80	5	NO	-	YES	-5.28
ArtUrban	80	60	5	NO	-	YES	-5.57
ArtUrban	80	50	5	NO	-	YES	-5.72
ArtUrban	80	30	5	NO	-	YES	-5.90
ArtUrban	50	100	5	NO	-	YES	-8.18
ArtUrban	50	80	5	NO	-	YES	-8.45
ArtUrban	50	60	5	NO	-	YES	-8.75
ArtUrban	50	50	5	NO	-	YES	-8.93
ArtUrban	50	30	5	NO	-	YES	-9.33

Table 5: ArtUrban simulation results

It is interesting to see how the ArtUrban driving cycle is successfully completed for all cases. In Table 5, only simulations for $\alpha = 5^{o}$ are shown, but simulations for $\alpha = 0^{o}$ were also conducted and similar solutions are obtained. This is consistent with common sense: if the most demanding case is completed without complications, it is logic to assume that the same will occurr with less demanding cases.

See Annexes A.1 for the extended version of the simulation results for ArtUrban driving cycle.

4.2 Artemis Road driving cycle

Most interesting results for the Artemis Road driving cycle are presented in the following pages. The speed profile desired is more demanding than the one in ArtUrban, as it reaches higher velocities.

SOH = 100%, SOC = 30%, α = 5º

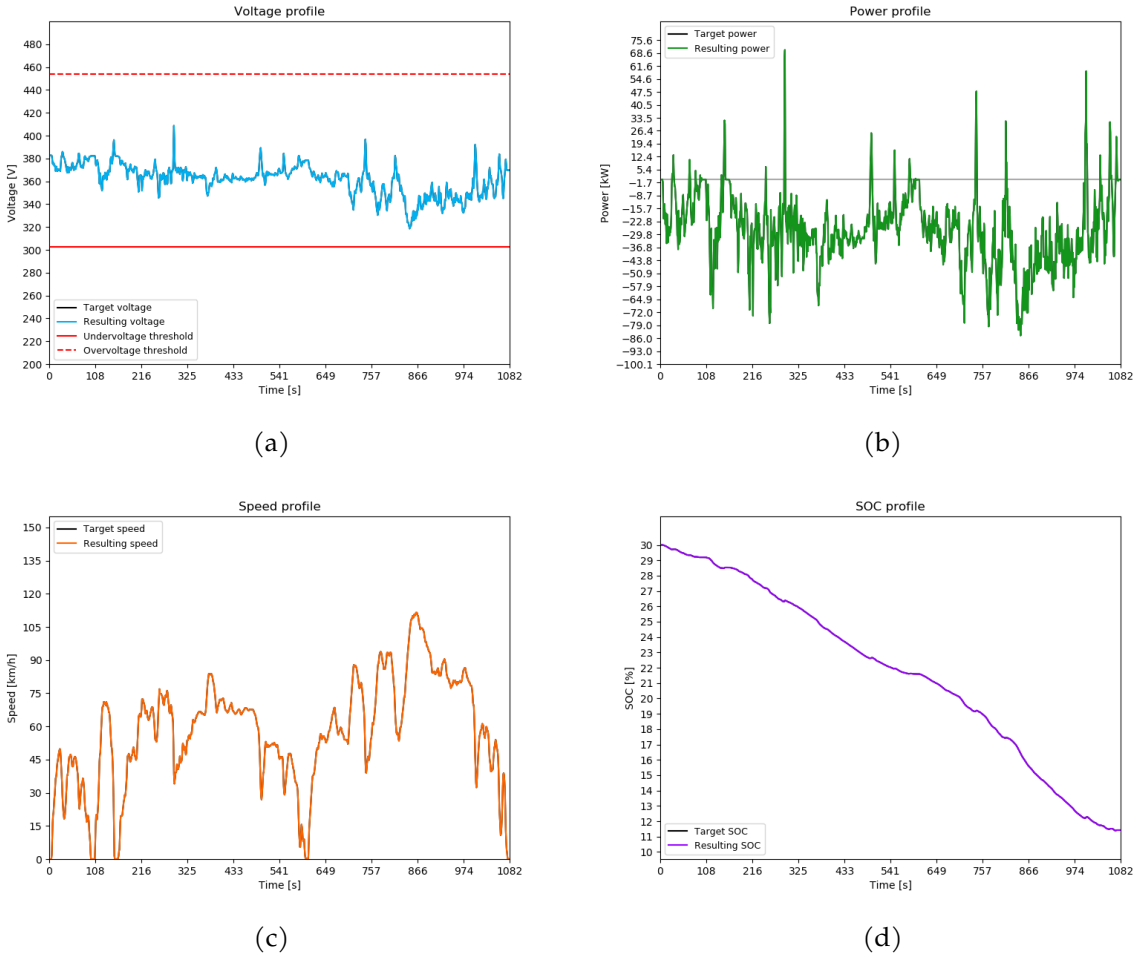

(a) (b)

(c) (d)

Figure 23: ArtRoad at SOH=100%, SOC=30%, α=5º

In this simulation we assume the battery to be at SOH=100%, which means that it has the characteristics of a brand new device. Despite the low initial SOC and an ArtRoad simulation at α= 5º, the EV is capable of finishing without needing BMS intervention and losing only 18.58% of SOC.

SOH = 50%, SOC = 30%, α = 5º

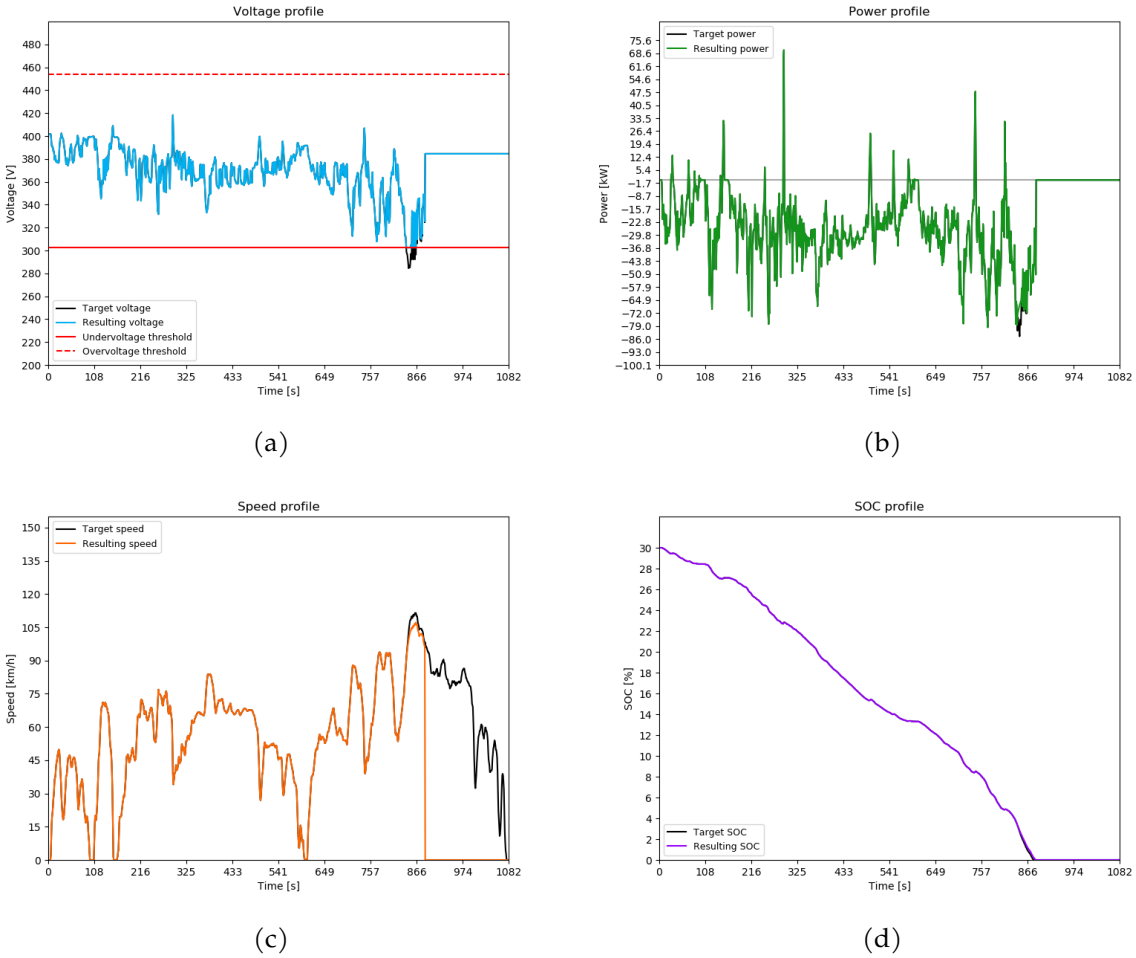

Figure 24: ArtRoad at SOH=50%, SOC=30%, α=5º

Under same road conditions and initial SOC as the case presented previously in Figure 23, it is observed that for lower SOH, the EV would not be able to finish the simulation successfully.

Undervoltage can be seen around second 800 of the simulation, and thus the BMS acts at this point by setting proper voltage levels. A result of this is seen both in the speed, power and SOC profiles. The power is modified as current is readjusted by the BMS as a consequence of the voltage reconfiguration. Lower power supplied by the battery results in speed decrease, which means that the user is not able to reach desired velocities due to the lower SOH constraint.

Another interesting fact is that the simulation cannot be completed due to SOC limitation, as the battery fully discharges before completing the driving cycle. Therefore, it is shown how the lower SOH also implies a faster SOC decrease.

SOH = 50%, SOC = 30%, α = 0º

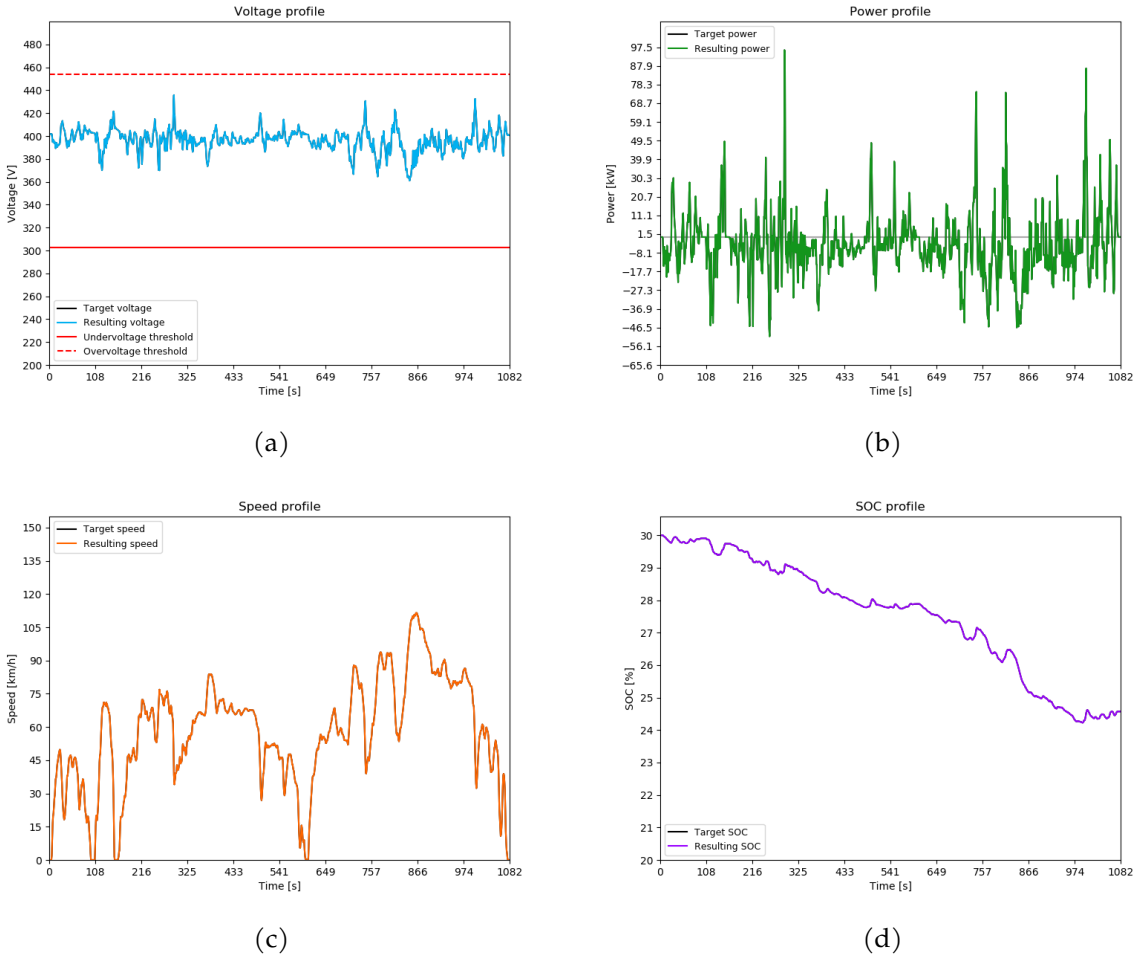

Figure 25: ArtRoad at SOH=50%, SOC=30%, α=0º

By exposing this simulation, it can be seen how the slope of the road affects the results. In this case, same battery conditions are the same as in Figure 24, but less steeper road means less demanding driving cycle, and as a consequence the simulation is completed with only a decrease of the SOC of 5.43%, and no undervoltage happening.

In Table 6, a summary of the most interesting results is shown. It is seen that within all simulations, undervoltage takes places only in the case where SOH=50%, SOC=30% and α=5º.

Driving cycle	SOH (%)	SOC (%)	Alpha (º)	Voltage Modified	Cause	Enough SOC	SOC Loss (%)
ArtRoad	50	30	5	YES	Undervoltage	NO	-30

Table 6: ArtRoad simulation results - Undervoltage

SOH = 100%, SOC = 100%, α = 0º

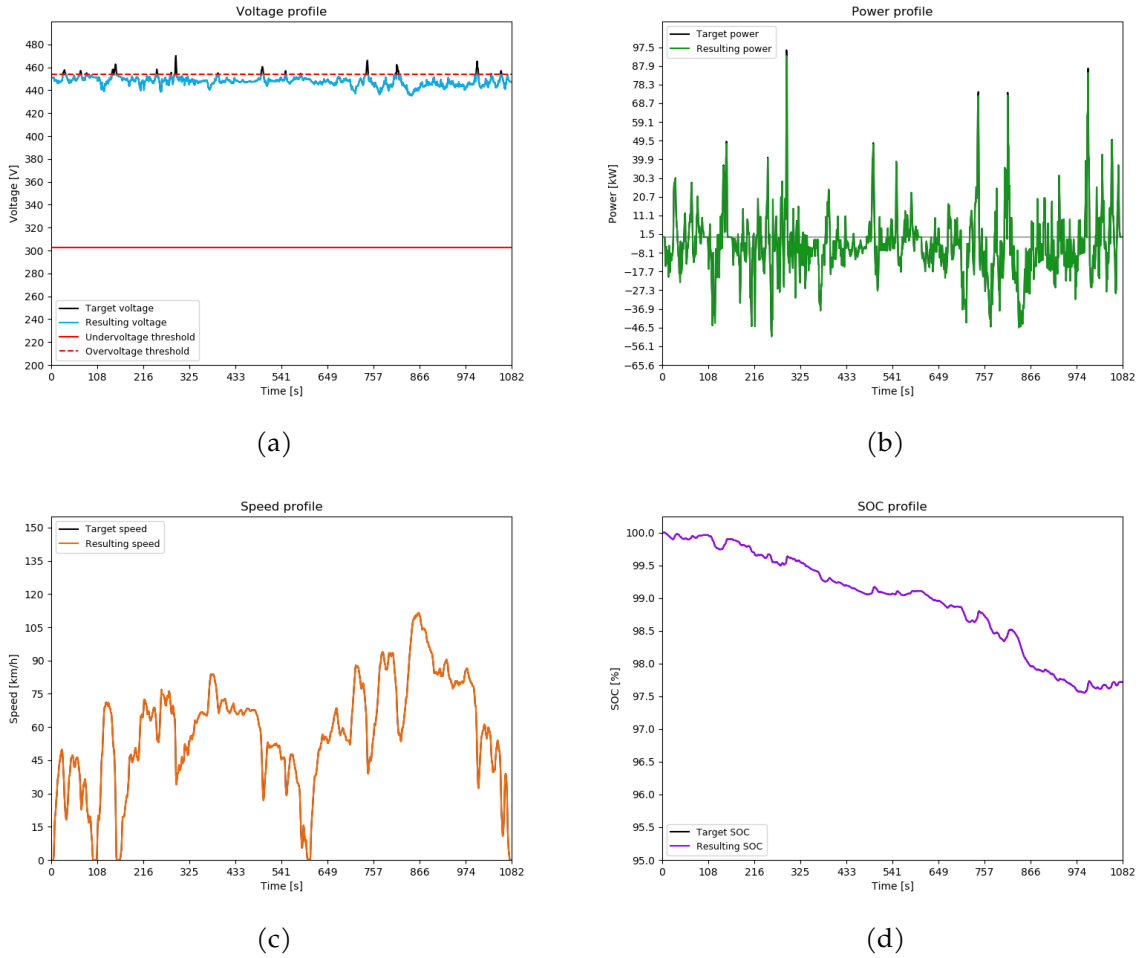

Figure 26: ArtRoad at SOH=100%, SOC=100%, α=0º

In this case of full SOH, SOC and α=0º, overvoltage occurs. This is because the SOC of the battery is already quite full, and decelerating makes regenerative breaking to provoke this overvoltage. Therefore, the BMS needs to take action but SOC and speed profile remain the same.

In Table 7 below, it is shown the cases in which overvoltage takes place. It is interesting to see how this happens at both road slope possible conditions and always when the SOC is at high levels. Additionally it is observed that overvoltage occurs also at lower SOC=80%, but only if the battery is degraded and has low SOH too.

Driving cycle	SOH (%)	SOC (%)	Alpha (º)	Voltage Modified	Cause	Enough SOC	SOC Loss (%)
ArtRoad	100	100	5	YES	Overvoltage	YES	-15.30
ArtRoad	80	100	5	YES	Overvoltage	YES	-19.41
ArtRoad	100	100	0	YES	Overvoltage	YES	-2.79
ArtRoad	80	100	0	YES	Overvoltage	YES	-3.40
ArtRoad	50	100	0	YES	Overvoltage	YES	-5.45
ArtRoad	50	80	0	YES	Overvoltage	YES	-4.86

Table 7: ArtRoad simulation results - Overvoltage

See Annexes A.2 for the extended version of the simulation results for ArtRoad driving cycle.

4.3 Artemis Motorway 130 driving cycle

Now, simulations for the Motorway driving cycle of variant 130 are shown. These simulations are interesting since the driving profile is much more demanding when higher velocities of 130 km/h are desired.

SOH = 100%, SOC = 50%, α = 5º

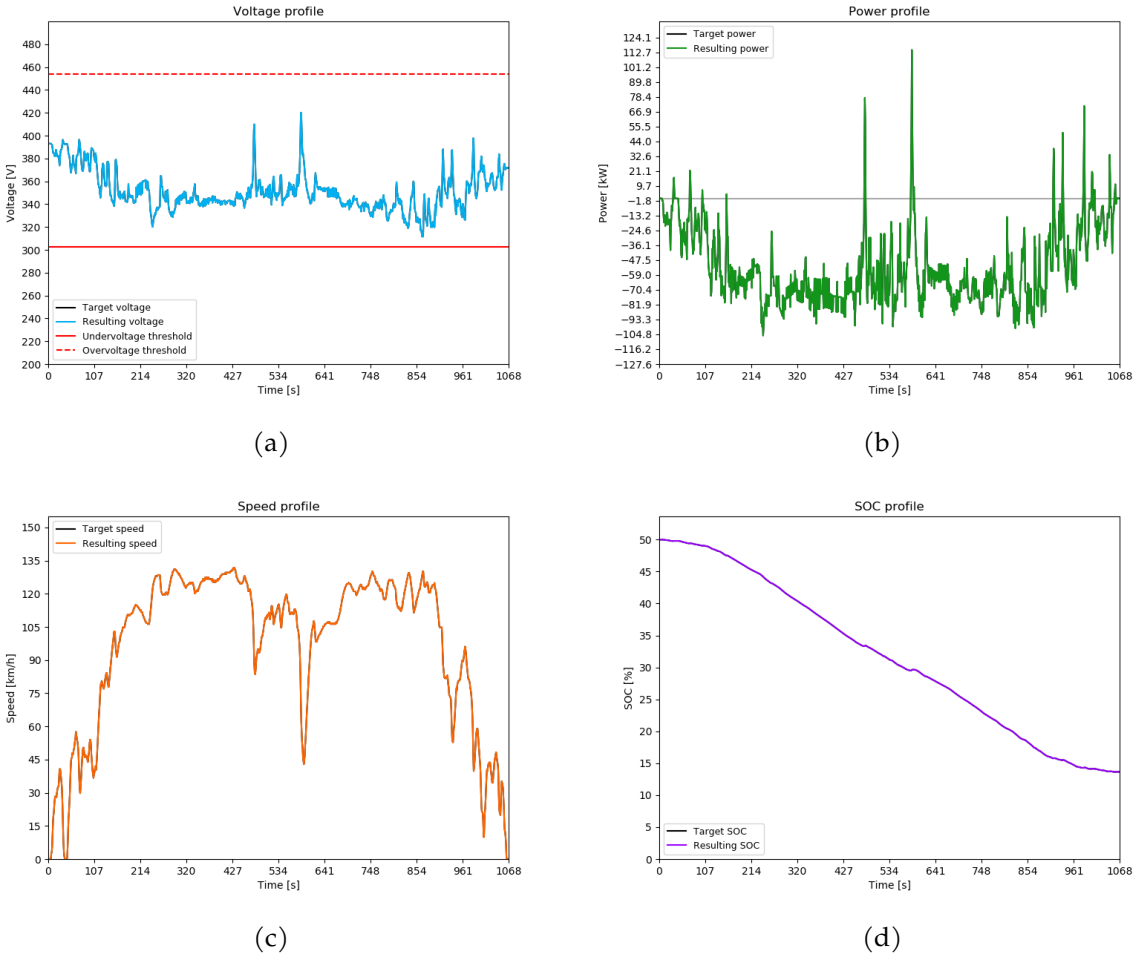

Figure 27: ArtMw130 at SOH=100%, SOC=50%, α=5º

Under these driving cycle conditions, the EV battery is able to complete the simulation without undervoltage but losing a 35.36% of SOC. It is then very likely that another ArtMw130 driving cycle would result in insufficient SOC if the same EV was to repeat the speed profile just after the one shown in Figure 27.

SOH = 80%, SOC = 50%, α = 5º

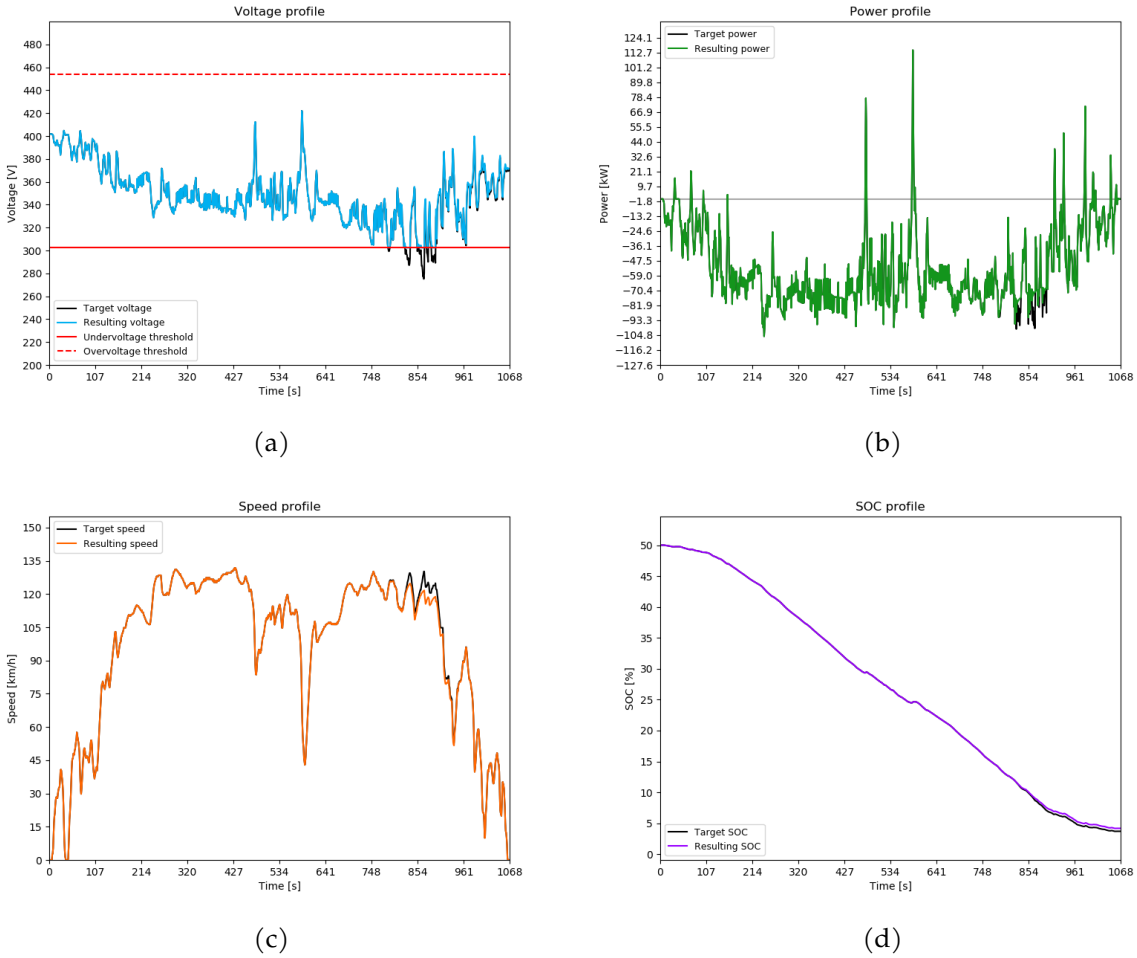

Figure 28: ArtMw130 at SOH=80%, SOC=50%, α=5º

If SOH is decreased and the battery is assumed to have now a 80% of SOH, for the same other conditions exposed in Figure 27 the EV is able to finish the driving cycle but BMS needs to intervene due to undervoltage, and speed is decreased at such instants of time. Additionally, there is a loss of 45.81% of the SOC.

SOH = 50%, SOC = 50%, α = 5º

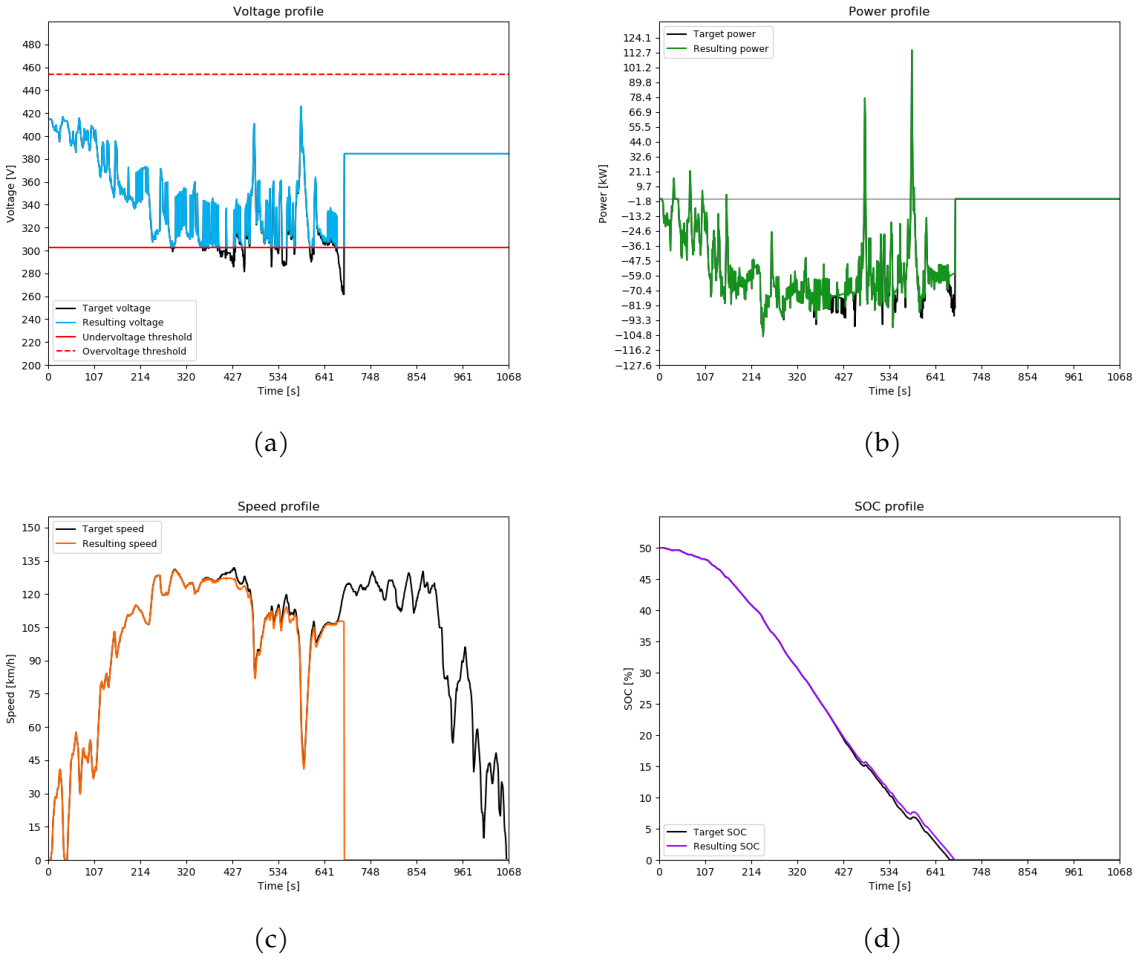

Figure 29: ArtMw130 at SOH=50%, SOC=50%, α=5º

Finally, if SOH is decreased even further to a 50%, it is seen that the car is no longer able to finish simulation due to such rapid loss of SOC. Additionally, there is more undervoltage and it even appears more rapidly compared to Figure 28.

ArtMw130 is a very suitable driving cycle in which it can be seen the impact of battery degradation in vehicle performance. A summary of most important simulations containing undervoltage can be seen in Table 8.

Driving cycle	SOH (%)	SOC (%)	Alpha (º)	Voltage Modified	Cause	Enough SOC	SOC Loss (%)
ArtMw130	90	50	5	YES	Undervoltage	YES	-40.64
ArtMw130	80	50	5	YES	Undervoltage	YES	-45.81
ArtMw130	70	60	5	YES	Undervoltage	YES	-52.38
ArtMw130	60	80	5	YES	Undervoltage	YES	-59.10
ArtMw130	60	70	5	YES	Undervoltage	YES	-60.53
ArtMw130	50	90	5	YES	Undervoltage	YES	-69.25
ArtMw130	50	80	5	YES	Undervoltage	YES	-71.06
ArtMw130	100	30	5	YES	Undervoltage	NO	-30
ArtMw130	90	30	5	YES	Undervoltage	NO	-30
ArtMw130	80	30	5	YES	Undervoltage	NO	-30
ArtMw130	70	50	5	YES	Undervoltage	NO	-50
ArtMw130	70	30	5	YES	Undervoltage	NO	-30
ArtMw130	60	60	5	YES	Undervoltage	NO	-60
ArtMw130	60	50	5	YES	Undervoltage	NO	-50
ArtMw130	60	30	5	YES	Undervoltage	NO	-30
ArtMw130	50	70	5	YES	Undervoltage	NO	-70
ArtMw130	50	60	5	YES	Undervoltage	NO	-60
ArtMw130	50	50	5	YES	Undervoltage	NO	-50
ArtMw130	50	30	5	YES	Undervoltage	NO	-30

Table 8: ArtMw130 simulation results - Undervoltage

Overvoltage also ocurrs in this driving cycle, and simulated cases where it takes place are seen in Table 9 below. It is appreciated again that overvoltage occurs at high initial SOC and when α=0º.

Driving cycle	SOH (%)	SOC (%)	Alpha (º)	Voltage Modified	Cause	Enough SOC	SOC Loss (%)
ArtMw130	100	100	0	YES	Overvoltage	YES	-8.13
ArtMw130	100	90	0	YES	Overvoltage	YES	-8.04
ArtMw130	90	100	0	YES	Overvoltage	YES	-9.07
ArtMw130	90	90	0	YES	Overvoltage	YES	-9.00
ArtMw130	90	80	0	YES	Overvoltage	YES	-9.17
ArtMw130	80	100	0	YES	Overvoltage	YES	-10.26
ArtMw130	80	90	0	YES	Overvoltage	YES	-10.19
ArtMw130	80	80	0	YES	Overvoltage	YES	-10.35
ArtMw130	70	100	0	YES	Overvoltage	YES	-11.81
ArtMw130	70	90	0	YES	Overvoltage	YES	-11.72
ArtMw130	70	80	0	YES	Overvoltage	YES	-11.90
ArtMw130	70	70	0	YES	Overvoltage	YES	-12.22
ArtMw130	60	100	0	YES	Overvoltage	YES	-13.87
ArtMw130	60	90	0	YES	Overvoltage	YES	-13.78
ArtMw130	60	80	0	YES	Overvoltage	YES	-13.98
ArtMw130	60	70	0	YES	Overvoltage	YES	-14.29
ArtMw130	50	100	0	YES	Overvoltage	YES	-16.70
ArtMw130	50	90	0	YES	Overvoltage	YES	-16.61
ArtMw130	50	80	0	YES	Overvoltage	YES	-16.82
ArtMw130	50	70	0	YES	Overvoltage	YES	-17.07
ArtMw130	50	60	0	YES	Overvoltage	YES	-17.42

Table 9: ArtMw130 simulation results - Overvoltage

See Annexes A.3 for the extended version of the simulation results for ArtMw130 driving cycle.

4.4 Artemis Motorway 150 driving cycle

SOH = 80%, SOC = 50%, α = 5º

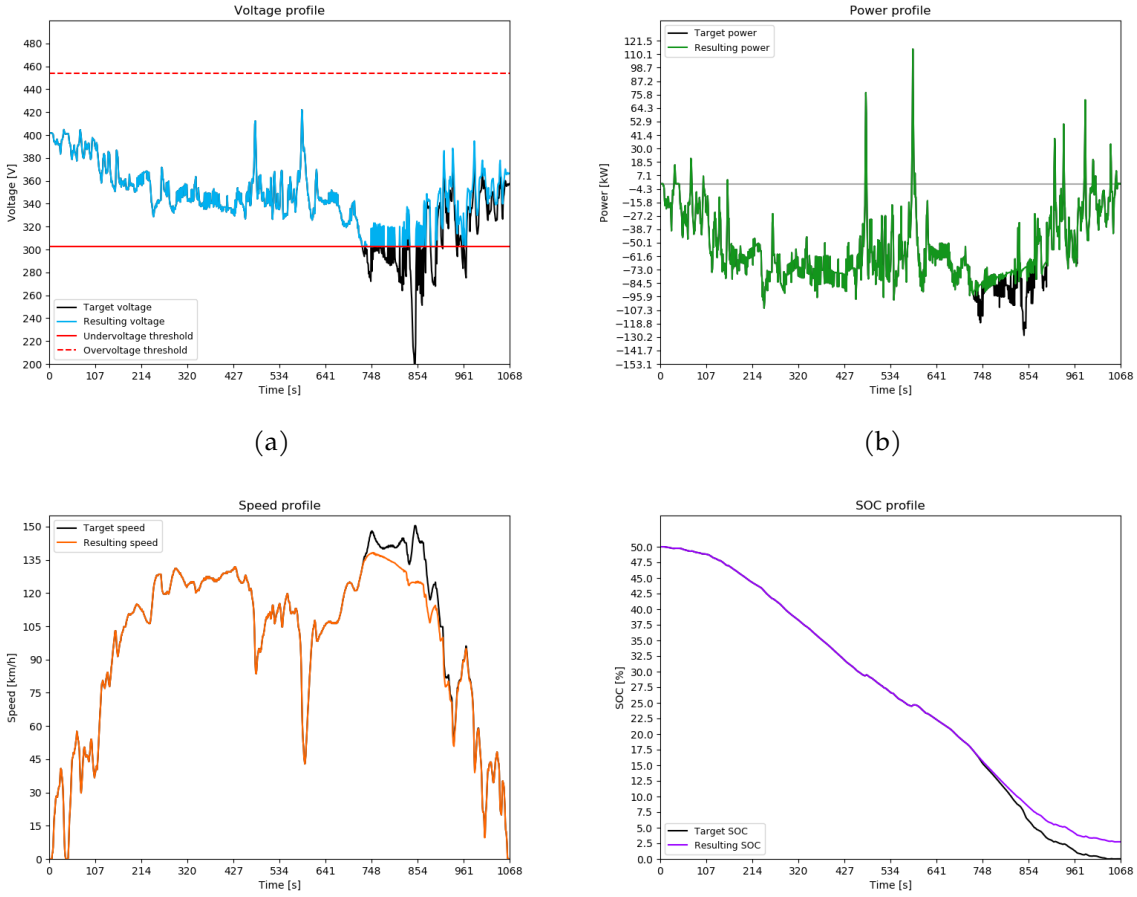

Figure 30: ArtMw150 at SOH=80%, SOC=50%, α=5º

It is observed that for a relatively high SOH of 80%, 50% of SOC and an α of 5º, the BMS needs to intervene for a considerable amount of time due to undervoltage. In fact, the differences between the response under ArtMw130 and ArtMw150 can be appreciated by comparing Figure 28 and Figure 30.

This simulation is also very interesting since it is seen that undervoltage occurs at highest velocities at the end of the simulation, which represent the most critical points. However when demanded velocity decreases, then the voltage is again within correct operational limits and the BMS intervention finishes. As a consequence, target and desired speed coincide again.

Additionally, it is easier to see the impact of the BMS on the SOC. If it did not exist, SOC would have reached 0%. However with the BMS, the SOC loss is smaller and simulation is finished with some remaining level of SOC thanks to the power reduction taking place when there is undervoltage.

SOH = 50%, SOC = 50%, α = 5º

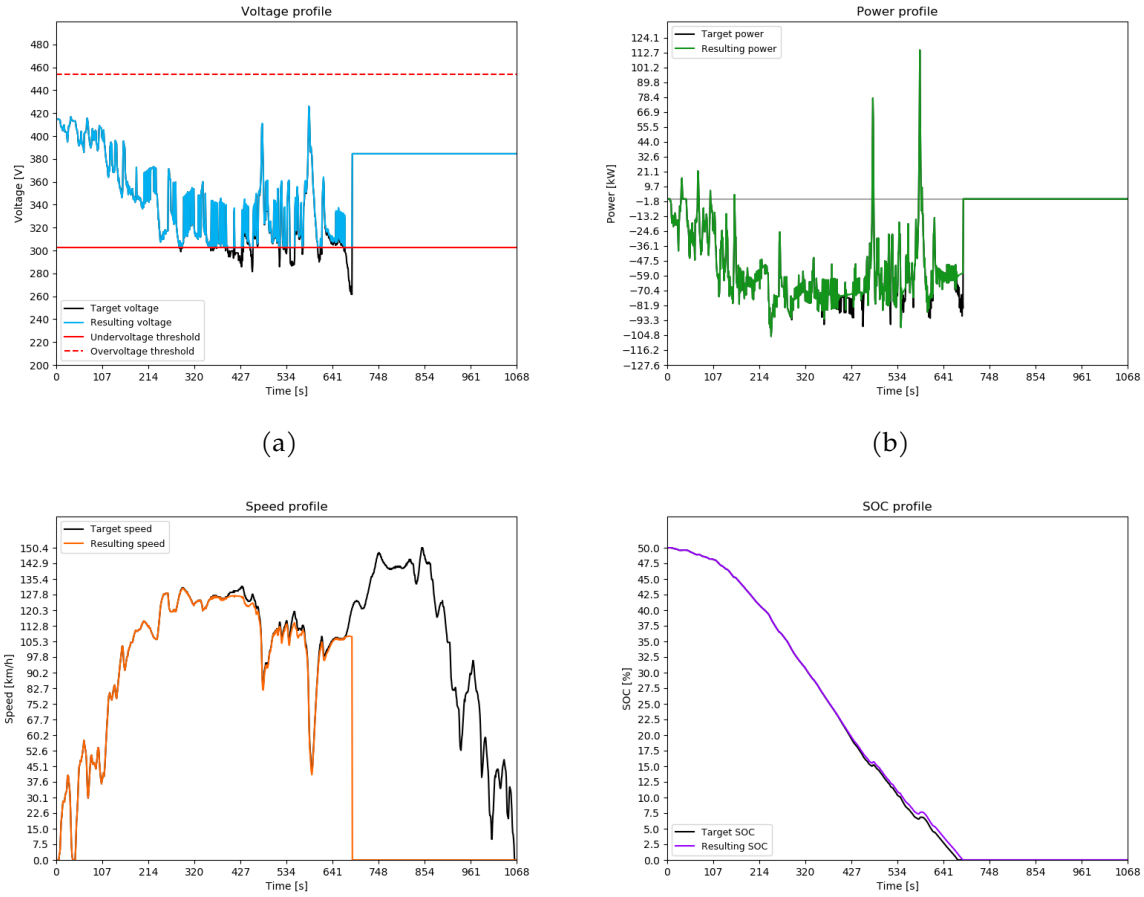

Figure 31: ArtMw150 at SOH=50%, SOC=50%, α=5º

Similarly to what happens in Figure 29, when SOH is decreased and the battery is more degraded, the simulation cannot longer finish due to lack of remaining SOC and undervoltage also appears earlier.

Table 10 shows a summary of all simulations where undervoltage appears for ArtMw150, and in Table 11 it can be seen all cases where there appered overvoltage.

Driving cycle	SOH (%)	SOC (%)	Alpha (º)	Voltage Modified	Cause	Enough SOC	SOC Loss (%)
ArtMw150	100	80	5	YES	Undervoltage	YES	-35.07
ArtMw150	100	50	5	YES	Undervoltage	YES	-38.41
ArtMw150	90	60	5	YES	Undervoltage	YES	-41.94
ArtMw150	90	50	5	YES	Undervoltage	YES	-42.68
ArtMw150	80	60	5	YES	Undervoltage	YES	-47.28
ArtMw150	80	50	5	YES	Undervoltage	YES	-47.25
ArtMw150	70	80	5	YES	Undervoltage	YES	-52.35
ArtMw150	70	60	5	YES	Undervoltage	YES	-53.76
ArtMw150	60	100	5	YES	Undervoltage	YES	-58.54
ArtMw150	60	80	5	YES	Undervoltage	YES	-61.46
ArtMw150	50	100	5	YES	Undervoltage	YES	-71.28
ArtMw150	50	80	5	YES	Undervoltage	YES	-72.78
ArtMw150	100	30	5	YES	Undervoltage	NO	-30
ArtMw150	90	30	5	YES	Undervoltage	NO	-30
ArtMw150	80	30	5	YES	Undervoltage	NO	-30
ArtMw150	70	50	5	YES	Undervoltage	NO	-50
ArtMw150	70	30	5	YES	Undervoltage	NO	-30
ArtMw150	60	60	5	YES	Undervoltage	NO	-60
ArtMw150	60	50	5	YES	Undervoltage	NO	-50
ArtMw150	60	30	5	YES	Undervoltage	NO	-30
ArtMw150	50	60	5	YES	Undervoltage	NO	-60
ArtMw150	50	50	5	YES	Undervoltage	NO	-50
ArtMw150	50	30	5	YES	Undervoltage	NO	-30

Table 10: ArtMw150 simulation results - Undervoltage

Driving cycle	SOH (%)	SOC (%)	Alpha (º)	Voltage Modified	Cause	Enough SOC	SOC Loss (%)
ArtMw150	100	100	0	YES	Overvoltage	YES	-8.93
ArtMw150	90	100	0	YES	Overvoltage	YES	-9.97
ArtMw150	90	80	0	YES	Overvoltage	YES	-10.13
ArtMw150	80	100	0	YES	Overvoltage	YES	-11.28
ArtMw150	80	80	0	YES	Overvoltage	YES	-11.45
ArtMw150	70	100	0	YES	Overvoltage	YES	-12.99
ArtMw150	70	80	0	YES	Overvoltage	YES	-13.19
ArtMw150	60	100	0	YES	Overvoltage	YES	-15.28
ArtMw150	60	80	0	YES	Overvoltage	YES	-15.51
ArtMw150	50	100	0	YES	Overvoltage	YES	-18.41
ArtMw150	50	80	0	YES	Overvoltage	YES	-18.65
ArtMw150	50	60	0	YES	Overvoltage	YES	-19.36

Table 11: ArtMw150 simulation results - Overvoltage

See Annexes A.4 for the extended version of the simulation results for ArtMw150 driving cycle.

4.5 Real Cycle

Finally, results for the Real Cycle simulation are presented. This driving cycle is of longer duration compared to the Artemis driving cycles. Thus the SOC loss will be greater for a given real cycle in comparison with the Artemis.

SOH = 100%, SOC = 70%, α = 5º

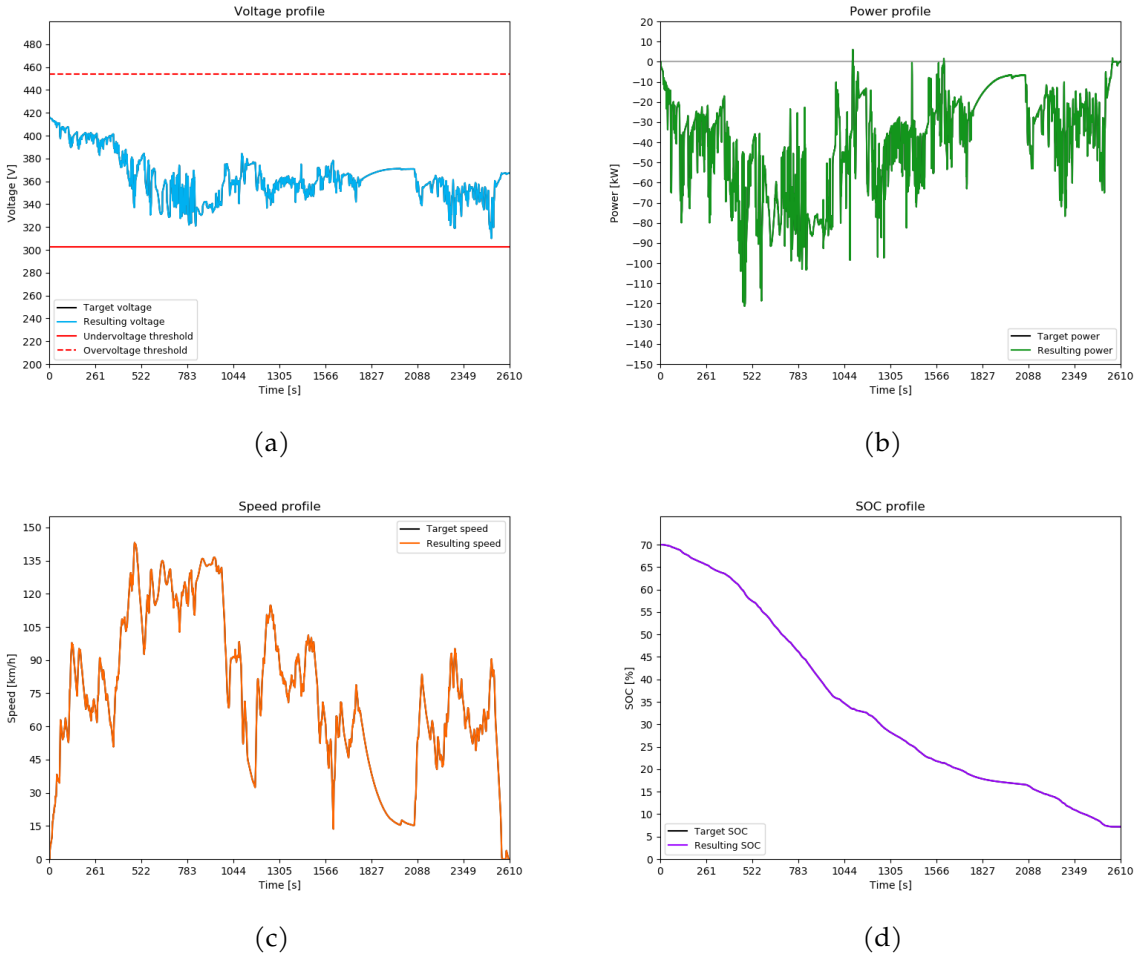

(a) (b)

(c) (d)

Figure 32: Real Cycle at SOH=100%, SOC=70%, α=5º

For the given initial conditions, it is obtained that the simulation for this particular real driving cycle can be completed without trouble as there is enough SOC to reach the end, and no undervoltage nor overvoltage occur.

SOH = 100%, SOC = 60%, α = 5º

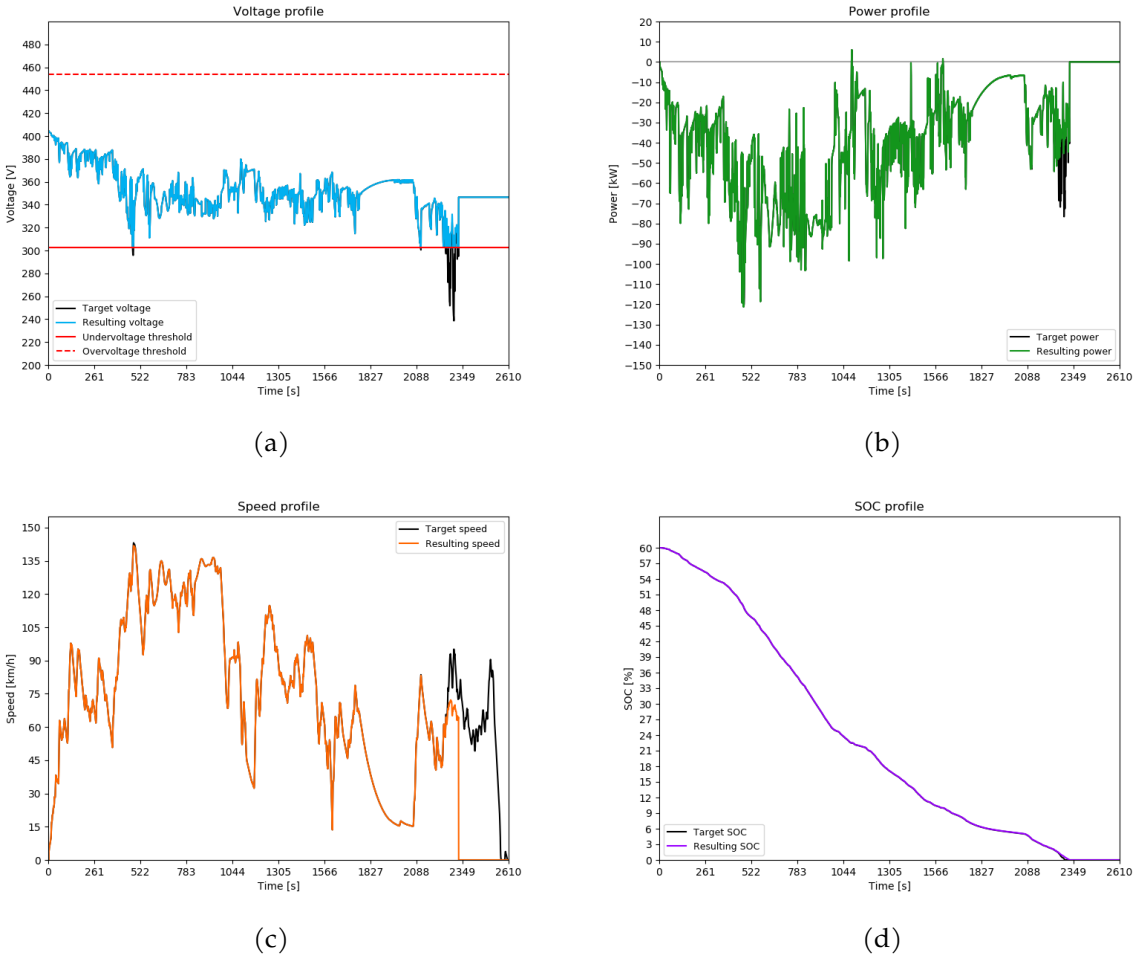

Figure 33: Real Cycle at SOH=100%, SOC=60%, α=5º

If the initial SOC is lowered to a 60%, the resulting simulation indicates that the SOC will not be enough to finish the real driving cycle. Additionally it will have undervoltage right before reaching a SOC=0%.

SOH = 90%, SOC = 70%, α = 5º

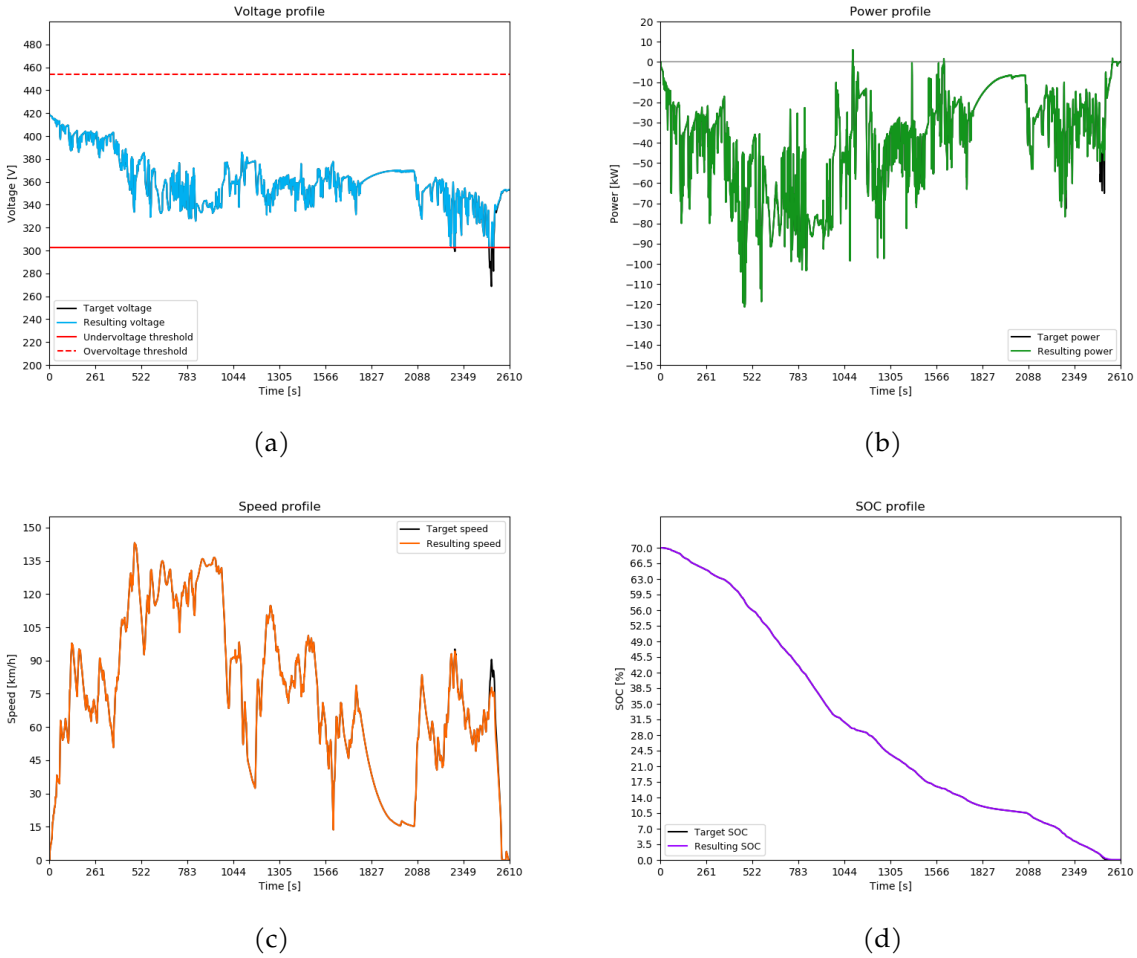

Figure 34: Real Cycle at SOH=90%, SOC=70%, α=5º

If the SOH is now 90% but all other conditions remain the same as in Figure 32, there appears undervoltage but the simulation is able to be finished, with a SOC of 0.05% at the end.

An interesting fact about the Real cycle profile is that it does not yield to overvoltage cases under any circumstances, unlike the Artemis driving cycles. Thus, simulations might have undervoltage or may not be able to finish due to a lack of enough SOC, but the BMS never needs to act to set lower voltages in case of exceeding levels of permited maximum voltages. In Table 12 all cases of undervoltage are presented, and in Table 13, cases where the BMS did not intervene but simulation could not finish either are also presented.

Driving cycle	SOH (%)	SOC (%)	Alpha (º)	Voltage Modified	Cause	Enough SOC	SOC Loss (%)
RealCycle	90	70	5	YES	Undervoltage	YES	-69.95
RealCycle	100	60	5	YES	Undervoltage	NO	-60
RealCycle	100	50	5	YES	Undervoltage	NO	-50
RealCycle	100	30	5	YES	Undervoltage	NO	-30
RealCycle	90	60	5	YES	Undervoltage	NO	-60
RealCycle	90	50	5	YES	Undervoltage	NO	-50
RealCycle	90	30	5	YES	Undervoltage	NO	-30
RealCycle	80	60	5	YES	Undervoltage	NO	-60
RealCycle	80	50	5	YES	Undervoltage	NO	-50
RealCycle	80	30	5	YES	Undervoltage	NO	-30
RealCycle	70	70	5	YES	Undervoltage	NO	-70
RealCycle	70	60	5	YES	Undervoltage	NO	-60
RealCycle	70	50	5	YES	Undervoltage	NO	-50
RealCycle	70	30	5	YES	Undervoltage	NO	-30
RealCycle	60	80	5	YES	Undervoltage	NO	-80
RealCycle	60	70	5	YES	Undervoltage	NO	-70
RealCycle	60	60	5	YES	Undervoltage	NO	-60
RealCycle	60	50	5	YES	Undervoltage	NO	-50
RealCycle	60	30	5	YES	Undervoltage	NO	-30
RealCycle	50	90	5	YES	Undervoltage	NO	-90
RealCycle	50	80	5	YES	Undervoltage	NO	-80
RealCycle	50	70	5	YES	Undervoltage	NO	-70
RealCycle	50	60	5	YES	Undervoltage	NO	-60
RealCycle	50	50	5	YES	Undervoltage	NO	-50
RealCycle	50	30	5	YES	Undervoltage	NO	-30

Table 12: RealCycle simulation results - Undervoltage

Driving cycle	SOH (%)	SOC (%)	Alpha (º)	Voltage Modified	Cause	Enough SOC	SOC Loss (%)
RealCycle	80	70	5	NO	-	NO	-70
RealCycle	70	80	5	NO	-	NO	-80
RealCycle	60	100	5	NO	-	NO	-100
RealCycle	60	90	5	NO	-	NO	-90
RealCycle	50	100	5	NO	-	NO	-100
RealCycle	50	30	0	NO	-	NO	-30

Table 13: RealCycle simulation results - Not enough SOC

See Annexes A.5 for the extended version of the simulation results for RealCycle driving cycle.

5 Discussion

With the resulting simulations, various aspects can be observed.

5.1 SOH level impact

The initial level of SOH of the battery determines the rate of discharge of the battery. As seen in Section 4, the healthier the battery is, the less SOC it loses throughout a simulation. The range of this relationship seems to be somehow proportional. That is, if the SOH is reduced to a half, then the SOC loss will be the double approximately.

For instance, it can be seen in Annexes A.5 that the SOC loss for the RealCycle at SOH=100%, SOC=80% and α=0º, is of 13.14% and the simulation ends with a remaining level of SOC of 66.86%. However, the same simulation with a SOH of 50% ends with a SOC of 53.50%, which means that there has been a SOC decrease of 26.50%.

This effect is the result of the changing battery ECM parameters depending on the SOH, and it implies that a battery with less SOH is more likely to fail in the middle of a driving cycle due to a lack of SOC. This is directly affecting the user, who may not be able to reach his or her destination. However, for non-steep roads, the user will not notice the low levels of SOH for not being able to reach desired speeds, as undervoltage and power reduction does not happen regardless of the SOH whenever α=0º.

5.2 SOC level impact

The SOC level also affects the SOC loss rate, but in a much more moderate amount. In other words, if the initial SOC is higher, the SOC loss will be lower, but differences within cases of different initial SOC are much smaller.

An example can be depicted with ArtMw150 simulations. In the particular case seen in Annexes A.4 of SOH=90%, SOC=100% and α=0º, the SOC decrease is of 9.97% and the simulation ends with a SOC of 90.03%. Hower, if same conditions apply but now the initial SOC is 30%, the SOC decrease is now of 11.54%, thus finishing the driving cycle with a SOC of 18.46%.

Therefore, the main impact that the SOC has on driving is not the varying rate SOC decrease, but whether the initial SOC is enough in order to terminate the simulation or not.

5.3 Road conditions impact

When α is 0º, the SOC loss is much lower than in steeped cases. Furthermore, in cases where there is no slope, only overvoltage appears if there are high initial SOC levels. This implies that the BMS intervention for power reduction does not take place for any driving cycle under these road circumstances and simulations not completed successfully are only due to a lack of initial SOC.

However, battery problems start to arise when there is a slope of 5º. The higher slope means that increased traction power is required to be delivered by the battery. In top of that, if determined speed and acceleration are desired, it is very likely that the BMS will invervene due to undervoltage, especially at lower initial SOC and at high velocities.

The enormous differences between having slope and not, seem to be of common sense. How-

ever, it must be remarked that simulations were assumed to have constant slope at all times, which may not be truly accurate for real-case scenarios. The 0º case could actually be accurate for very plain areas in determined countries. For instance, the Netherlands are famous for their very flat terrain. Nevertheless, mountainous landscapes would be more in line with the 5º slope cases. Still, a constant positive slope in areas having hills and valleys is a pretty strong assumption, as the slope profile is very likely to be variable with positive and negative slopes. In Figure 35, a road with 5º of slope is presented and by assuming a constant steepness of 5 degrees, extreme cases can be evaluated.

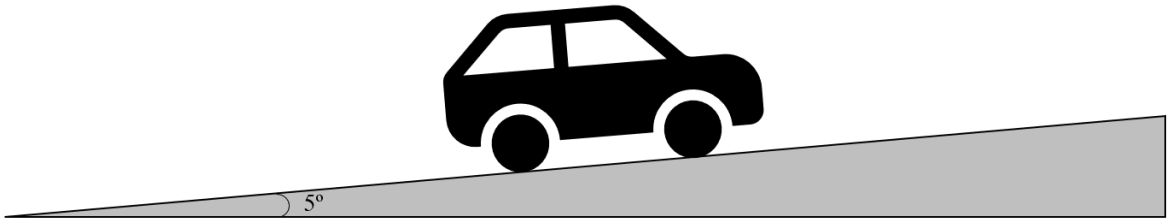

Figure 35: Road with 5º of slope

6 Project analysis

6.1 Temporal planning

A temporal Gantt chart can be seen in Figure 36. In it, it is indicated the main tasks done to conduct this thesis and the duration of each.

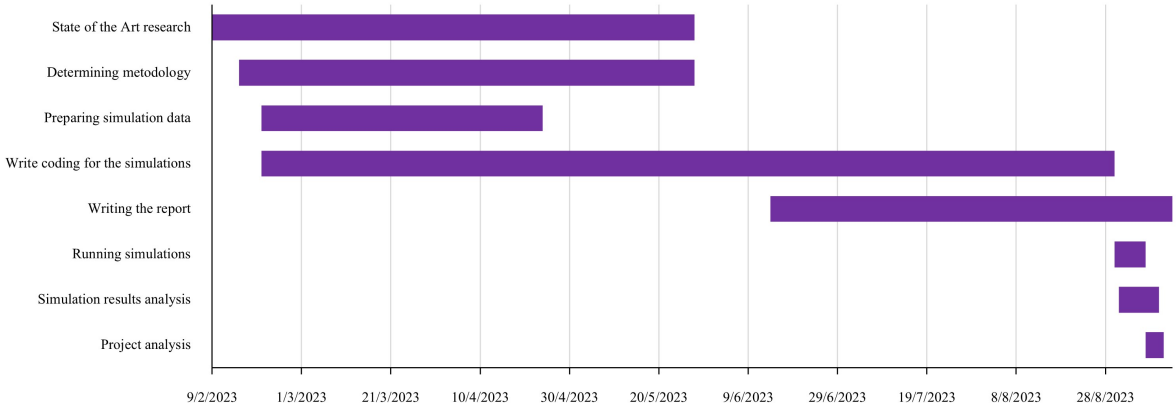

Figure 36: Gantt chart

6.2 Economic study

The project has consisted in making simulations with Python. To achieve so, the most crucial material resource was a computer which requires electricity so as to be functional.

In order to achieve the objectives of the project, investigation was needed to be done at the beginning of the thesis to understand the state of the art. All of the research was done electronically by using the Internet, and it is estimated that a total of 80 hours were required. Estimation is done by adding up shifts of various duration each that took place during the whole thesis development.

After the research, Python code was needed to be prepared to start simulations. Coding took about 200 hours in total. Within that time, codes for preparation of data (initial interpolation and extrapolation of the battery parameters), driving cycles data treatment, trial-error coding for reaching to the final script, and plots recompilation of the achieved results are included.

When the final code was achieved, a total of 288 simulations of the different driving cycles were done to collect enough data that could lead to meaningful conclusions. Each simulation lasted an average time of 20 minutes each. Thus, the simulations solely required the computer to be operating a total time of 96 hours.

Finally, writing the thesis report and presenting the simulation results took about 70 hours.

By taking into account that the so mentioned tasks were all done by the computer, it is obtained that this device has been operating for 446 hours approximately. The computer used for the project has a power of 45 W, which means that the total power consumption is of 20.07 kWh. Assuming that the average price of electricity in Spain (the country where the project is held) during the last 7 months (the duration of developing the project) has been of about 0.2€/kWh

approximately, then the total electricity cost adds up to approximately 4€.

Another very important aspect to take into account when referring to costs is the time invested in the project in order to develop it. Only 2 people were involved in the making process: the mentor and the student, who organized weekly meetings of around 30 minutes each for 30 weeks.

Regarding the mentor side, it is important to bear in mind that an average salary of a university professor in Spain is around 2500€ at full-time, which yields that the hourly salary is around 15.6€/hour. Considering weekly meetings, responsibility of mentoring the project, and extra hours that the tutor has invested in correcting report versions, it is obtained that the mentor work has resulted in a cost of approximately 500€ to the thesis.

No other extra costs are considered, since the student did not receive any salary to develop this thesis, consulted scientific papers were all open to the public, and the program used to code in Python can be downloaded for free.

Having everything into account, it is concluded that the thesis development has had a cost of approximately 504€.

6.3 Social study

The social impact of this thesis is based on the improvement of electromobility. This field highly benefits the quality of life of people, as EVs do not release greenhouse emissions. As a result, air is cleaner and the health of citizens is improved, especially for areas with high density of traffic and car usage levels.

Also, the vehicle model considered for this thesis is a relatively economical one in comparison with other famous competitors in the market. This was intended since the transition to electromobility needs to imply all sectors in our modern societies. If EVs have elevated prices, only those with higher incomes and patrimony will be able to access to them, and the collective benefits from EVs will be limited.

6.4 Environmental study

The negative environmental impact that this thesis has had only involves the electricity consumption occurred when charging the computer. However, it is pretty obvious that the project is quite environmentally friendly since it has not involved the usage of any raw material and therefore no waste has been generated.

Moreover, the thesis is motivated by environmental issues related to the reduction of greenhouse gas emissions. It looks over the future by investigating and studying EV vehicles, the core of electromobility.

Finally, it is seen that lifespan of the batteries could be extended as their performance is affected due to degradation but they still perform well enough to be considered as usable at lower SOH levels. A strong environmental benefit could be achieved if this was implemented because battery production levels would decrease. If this occurred, activities impacting on the environment such as waste generation and the extraction of raw materials (for instance lithium in our case) to build the batteries would decrease, as well as the resources spent on their manufacturing and

commercialization such as electricity, water, etc.

6.5 Gender study

This thesis content does not have much in common with gender or gender identity since electric vehicles, batteries and Python simulations do not refer to gender-related issues at any point.

Nevertheless, gender disparity can be studied concerning the people involved in the thesis development.

When considering the references employed in this project, particularly the scholarly works authored by experts that serve as the foundation of knowledge on the subject, it is notable that only 13.85% of these contributions are attributed to women, as seen in Figure 37. In fact, about a 64.5% of the consulted papers are exclusively written by men.

This is consistent with studies that reveal that female representation in the engineering field is significantly low compared to men, representing only a 9.8% according to [12].

Despite the big contribution disparity between genders for the cited articles, it is important to remark that this project was mentored by a woman and conducted by another one. Therefore, a total of 100% of people involved in the realization of this project corresponds to the female side.

Moreover, studies reveal that female representation is starting to change, adopting a growing trend. For example, a total of 24.5% students in the faculty of Escola Tècnica Superior d'Enginyeria Industrial de Barcelona during the academic year 2021-2022 were women. This suggests that gender roles are slowly breaking down, and women are nowadays more likely to access to STEM fields that one day were only dominated by men.

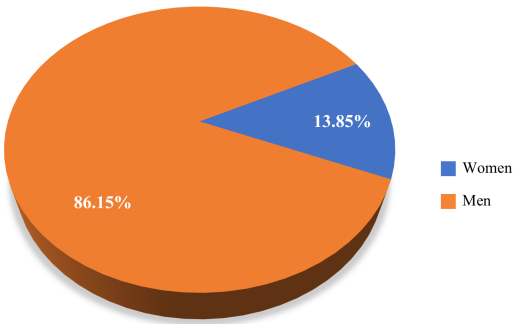

Figure 37: Gender disparity in authorship of the thesis citations

7 Conclusions and Future work

Project objectives have been achieved successfully and the following conclusions are obtained from the simulations.

It is obtained that the SOH of an EV battery does affect driving negatively as the battery discharge rate increases. However, batteries with a SOH lower than 80% could also achieve good performance in the sense that they are still capable of completing driving cycles successfully, especially under low-demanding driving conditions. Therefore, it is concluded that the end of life of the battery could be reconsidered and set to lower SOH levels according to our results, especially for users who do not make an intensive use of the vehicle or for those who live in flat areas. By doing so, multiple benefits could be obtained as the user could save up money by extending the life of the vehicle instead of buying a new one. Additionally, it would benefit the planet since battery production could be reduced and with it, environmental impact resulting from this activity such as mining for raw materials and energy consumption would be reduced to a lower extent.

Despite the reached conclusions, limitations of the project exist and must be recognised. The most important one is that temperature effects are completely disregarded and obtained conclusions could be highly affected due to this assumption. Moreover, the SOH has been considered to be constant, which may not be exactly true in real life. In order to improve the thesis and obtain more accurate results, temperature and SOH behaviour should be taken into account and included in equations to describe its impact.

Also, a slope profile could be implemented so as to have a more realistic simulation. This could be characterised by different slope angles at every time instant, and various profiles may also be done to represent mountaneous landscapes with more slope dimensions and variations, or flatter areas with smaller slope ranges.

Additionally, the ECM parameters were extrapolated at high levels of SOH. The assumption that these values were valid could be further studied, maybe with an experimental setup or by conducting simulations that modelled the behaviour of each battery cell at a chemical level.

Acknowledgments

First of all I would like to thank to all my friends and family all their unconditional support. To my mother and grandmother, for their trust in me and for being my flashlights during the thesis development and the whole Bachelor's degree. To Sergi, for his kindness and care which have truly been a source of strength and comfort when difficult times arose. And to my best friends, who have always stayed by my side regardless of the circumstances. Without each one of you, this journey would have been considerably more arduous. Your support and belief in me have made all the difference.

Finally, I would like to extend my thanks to my tutor Maite for all her mentoring, patience and knowledge provided along all this journey. She has been truly helpful and very much needed guidance was provided throughout the project's ups and downs.

Bibliography

[1] Lorenzo Berzi, Massimo Delogu, and Marco Pierini. Development of driving cycles for electric vehicles in the context of the city of florence. *Transportation Research Part D: Transport and Environment*, 47:299–322, 2016.

[2] R Borah, FR Hughson, J Johnston, and T Nann. On battery materials and methods. *Materials Today Advances*, 6:100046, 2020.

[3] José Cabrera, Aurelio Vega, Félix Tobajas, Víctor Déniz, and Himar A Fabelo. Design of a reconfigurable li-ion battery management system (bms). In *2014 XI Tecnologias Aplicadas a la Ensenanza de la Electronica (Technologies Applied to Electronics Teaching)(TAEE)*, pages 1–6. IEEE, 2014.

[4] Ching Chuen Chan. The state of the art of electric and hybrid vehicles. *Proceedings of the IEEE*, 90(2):247–275, 2002.

[5] Lee Chapman. Transport and climate change: a review. *Journal of Transport Geography*, 15(5):354–367, September 2007.

[6] RM Dell. Batteries: fifty years of materials development. *Solid State Ionics*, 134(1-2):139–158, 2000.

[7] Jing Deng, Kang Li, David Laverty, Weihua Deng, and Yusheng Xue. Li-ion battery management system for electric vehicles-a practical guide. In *Intelligent Computing in Smart Grid and Electrical Vehicles: International Conference on Life System Modeling and Simulation, LSMS 2014 and International Conference on Intelligent Computing for Sustainable Energy and Environment, ICSEE 2014 Shanghai, China, September 20-23, 2014 Proceedings, Part III*, pages 32–44. Springer, 2014.

[8] Yuanli Ding, Zachary P Cano, Aiping Yu, Jun Lu, and Zhongwei Chen. Automotive li-ion batteries: current status and future perspectives. *Electrochemical Energy Reviews*, 2:1–28, 2019.

[9] Boucar Diouf and Ramchandra Pode. Potential of lithium-ion batteries in renewable energy. *Renewable Energy*, 76:375–380, 2015.

[10] Jacqueline S. Edge, Simon O'Kane, Ryan Prosser, Niall D. Kirkaldy, Anisha N. Patel, Alastair Hales, Abir Ghosh, Weilong Ai, Jingyi Chen, Jiang Yang, Shen Li, Mei-Chin Pang, Laura Bravo Diaz, Anna Tomaszewska, M. Waseem Marzook, Karthik N. Radhakrishnan, Huizhi Wang, Yatish Patel, Billy Wu, and Gregory J. Offer. Lithium ion battery degradation: what you need to know. *Physical Chemistry Chemical Physics*, 23(14):8200–8221, 2021.

[11] A Esteves-Booth, T Muneer, J Kubie, and H Kirby. A review of vehicular emission models and driving cycles. *Proceedings of the Institution of Mechanical Engineers, Part C: Journal of Mechanical Engineering Science*, 216(8):777–797, 2002.

[12] Daniel J Foley. Characteristics of doctoral scientists and engineers in the united states: 2006. detailed statistical tables. nsf 09-317. *National Science Foundation*, 2009.

[13] Hossam A Gabbar, Ahmed M Othman, and Muhammad R Abdussami. Review of battery management systems (bms) development and industrial standards. *Technologies*, 9(2):28, 2021.

[14] Jürgen Garche, Chris K Dyer, Patrick T Moseley, Zempachi Ogumi, David AJ Rand, and Bruno Scrosati. *Encyclopedia of electrochemical power sources*. Newnes, 2013.

[15] Omer Faruk Goksu, Ahmet Yigit Arabul, and Revna Acar Vural. Low voltage battery management system with internal adaptive charger and fuzzy logic controller. *Energies*, 13(9):2221, 2020.

[16] Wang Haiying, He Long, Sun Jianhua, Liu Shuanquan, and Wu Feng. Study on correlation with soh and eis model of li-ion battery. In *Proceedings of 2011 6th International Forum on Strategic Technology*, volume 1, pages 261–264. IEEE, 2011.

[17] David E Hall and J Cal Moreland. Fundamentals of rolling resistance. *Rubber chemistry and technology*, 74(3):525–539, 2001.

[18] Yong-Min Jeong, Yong-Ki Cho, Jung-Hoon Ahn, Seung-Hee Ryu, and Byoung-Kuk Lee. Enhanced coulomb counting method with adaptive soc reset time for estimating ocv. In *2014 IEEE Energy Conversion Congress and Exposition (ECCE)*, pages 1313–1318. IEEE, 2014.

[19] Hao Ji, Wei Zhang, Xu-Hai Pan, Min Hua, Yi-Hong Chung, Chi-Min Shu, and Li-Jing Zhang. State of health prediction model based on internal resistance. *International Journal of Energy Research*, 44(8):6502–6510, 2020.

[20] Olof Juhlin. Modeling of Battery Degradation in Electrified Vehicles.

[21] M Mastali, J Vazquez-Arenas, R Fraser, M Fowler, S Afshar, and M Stevens. Battery state of the charge estimation using kalman filtering. *Journal of Power Sources*, 239:294–307, 2013.

[22] Hyung-Joo Noh, Sungjune Youn, Chong Seung Yoon, and Yang-Kook Sun. Comparison of the structural and electrochemical properties of layered li [nixcoymnz] o2 (x= 1/3, 0.5, 0.6, 0.7, 0.8 and 0.85) cathode material for lithium-ion batteries. *Journal of power sources*, 233:121–130, 2013.

[23] Sabine Piller, Marion Perrin, and Andreas Jossen. Methods for state-of-charge determination and their applications. *Journal of power sources*, 96(1):113–120, 2001.

[24] Gregory L Plett. *Battery management systems, Volume I: Battery modeling*, volume 1. Artech House, 2015.

[25] Valer Pop, Henk Jan Bergveld, Dmitry Danilov, Paul PL Regtien, and Peter HL Notten. *Battery management systems: Accurate state-of-charge indication for battery-powered applications*, volume 9. Springer Science & Business Media, 2008.

[26] Bernd Propfe, Martin Redelbach, Danilo J Santini, and Horst Friedrich. Cost analysis of plug-in hybrid electric vehicles including maintenance & repair costs and resale values. *World Electric Vehicle Journal*, 5(4):886–895, 2012.

[27] Changsheng Qiu, Gang He, Wankai Shi, Mengjie Zou, and Chang Liu. The polarization

characteristics of lithium-ion batteries under cyclic charge and discharge. *Journal of Solid State Electrochemistry*, 23:1887–1902, 2019.

[28] Pedro V.H. Seger, Eddy Coron, Pierre-Xavier Thivel, Delphine Riu, Mikael Cugnet, and Sylvie Genies. Open data model parameterization of a second-life Li-ion battery. *Journal of Energy Storage*, 47:103546, March 2022.

[29] Emilia Silvas, Kobus Hereijgers, Huei Peng, Theo Hofman, and Maarten Steinbuch. Synthesis of realistic driving cycles with high accuracy and computational speed, including slope information. *IEEE Transactions on Vehicular Technology*, 65(6):4118–4128, 2016.

[30] Stefan Skoog. Parameterization of equivalent circuit models for high power lithium-ion batteries in HEV applications. In *2016 18th European Conference on Power Electronics and Applications (EPE'16 ECCE Europe)*, pages 1–10, Karlsruhe, September 2016. IEEE.

[31] Fuad Un-Noor, Sanjeevikumar Padmanaban, Lucian Mihet-Popa, Mohammad Nurunnabi Mollah, and Eklas Hossain. A comprehensive study of key electric vehicle (ev) components, technologies, challenges, impacts, and future direction of development. *Energies*, 10(8):1217, 2017.

[32] Yujie Wang, Jiaqiang Tian, Zhendong Sun, Li Wang, Ruilong Xu, Mince Li, and Zonghai Chen. A comprehensive review of battery modeling and state estimation approaches for advanced battery management systems. *Renewable and Sustainable Energy Reviews*, 131:110015, 2020.